



## The collection 5 MODIS burned area product – Global evaluation by comparison with the MODIS active fire product

D.P. Roy <sup>a,\*</sup>, L. Boschetti <sup>b</sup>, C.O. Justice <sup>b</sup>, J. Ju <sup>a</sup>

<sup>a</sup> Geographic Information Science Center of Excellence, South Dakota State University, Wecota Hall, Box 506B, Brookings, SD 57007, USA

<sup>b</sup> Department of Geography, University of Maryland, 2181 LeFrak Hall, College Park, MD 20740, USA

### ARTICLE INFO

#### Article history:

Received 23 December 2007

Received in revised form 19 May 2008

Accepted 24 May 2008

#### Keywords:

Fire  
Fire affected area  
Burned area  
MODIS  
Reporting

### ABSTRACT

The results of the first consecutive 12 months of the NASA Moderate Resolution Imaging Spectroradiometer (MODIS) global burned area product are presented. Total annual and monthly area burned statistics and missing data statistics are reported at global and continental scale and with respect to different land cover classes. Globally the total area burned labeled by the MODIS burned area product is  $3.66 \times 10^6 \text{ km}^2$  for July 2001 to June 2002 while the MODIS active fire product detected for the same period a total of  $2.78 \times 10^6 \text{ km}^2$ , i.e., 24% less than the area labeled by the burned area product. A spatio-temporal correlation analysis of the two MODIS fire products stratified globally for pre-fire leaf area index (LAI) and percent tree cover ranges indicate that for low percent tree cover and LAI, the MODIS burned area product defines a greater proportion of the landscape as burned than the active fire product; and with increasing tree cover ( $>60\%$ ) and LAI ( $>5$ ) the MODIS active fire product defines a relatively greater proportion. This pattern is generally observed in product comparisons stratified with respect to land cover. Globally, the burned area product reports a smaller amount of area burned than the active fire product in croplands and evergreen forest and deciduous needleleaf forest classes, comparable areas for mixed and deciduous broadleaf forest classes, and a greater amount of area burned for the non-forest classes. The reasons for these product differences are discussed in terms of environmental spatio-temporal fire characteristics and remote sensing factors, and highlight the planning needs for MODIS burned area product validation.

© 2008 Elsevier Inc. All rights reserved.

### 1. Introduction

Mapping the timing and extent of fires is important as fire is a prominent disturbance factor affecting ecosystem structure and the cycling of carbon and nutrients and is a globally-significant cause of greenhouse gas emissions (e.g., Crutzen & Andreae, 1990; Bond et al., 2005). There is a growing debate on the relationship between fire and climate change (Weber and Flannigan, 1997; Siegert et al., 2001; Alencar et al., 2006; Westerling et al., 2006; Denman et al., 2007) and a perceived increasing incidence, extent, and severity of uncontrolled burning globally that has lead to calls for international environmental policy concerning fire (FAO, 2007).

Satellite data have been used to monitor biomass burning at regional to global scale for more than two decades using algorithms that detect the location of active fires at the time of satellite overpass, and in the last decade using burned area mapping algorithms that map directly the spatial extent of the areas affected by fires. The NASA Moderate Resolution Imaging Spectroradiometer (MODIS) on the

Terra (morning) and Aqua (afternoon) satellites has specific features for fire monitoring and has been used to systematically generate a suite of global MODIS land products (Justice et al., 2002b) including a 1 km active fire product (Kaufman et al., 1998; Justice et al., 2002a; Giglio et al., 2003) and more recently a burned area product that maps the approximate day and extent of burning at 500 m resolution (Roy et al., 2005a). The MODIS burned area product was developed and tested only on a regional basis using data from Collection 1 (Roy et al., 2002a) and Collection 4 (Roy et al., 2005a). This collection numbering scheme is used to differentiate between different MODIS represcussions, each applying the latest available version of the science algorithms to the MODIS instrument data and using the best available calibration and geolocation information (Masuoka et al. in press). The first global burned area product is now being generated as part of the MODIS Land Collection 5 product suite and is currently available, with supporting information, from the MODIS Fire website ([WWW1](http://WWW1)).

This paper describes a global assessment of the Collection 5 MODIS burned area product. It is commonly accepted that satellite derived active fire products are less suitable for assessing area burned than products generated by direct mapping of area burned; for this reason, in the absence of accurate burned area products, previously, burned area assessments have been created based on calibrating the available active fire data from regional AVHRR (Scholes et al., 1996) and global

\* Corresponding author.

E-mail addresses: [david.roy@sdstate.edu](mailto:david.roy@sdstate.edu) (D.P. Roy), [lugi.boschetti@hermes.geog.umd.edu](mailto:lugi.boschetti@hermes.geog.umd.edu) (L. Boschetti), [justice@hermes.geog.umd.edu](mailto:justice@hermes.geog.umd.edu) (C.O. Justice), [junchang.ju@sdstate.edu](mailto:junchang.ju@sdstate.edu) (J. Ju).

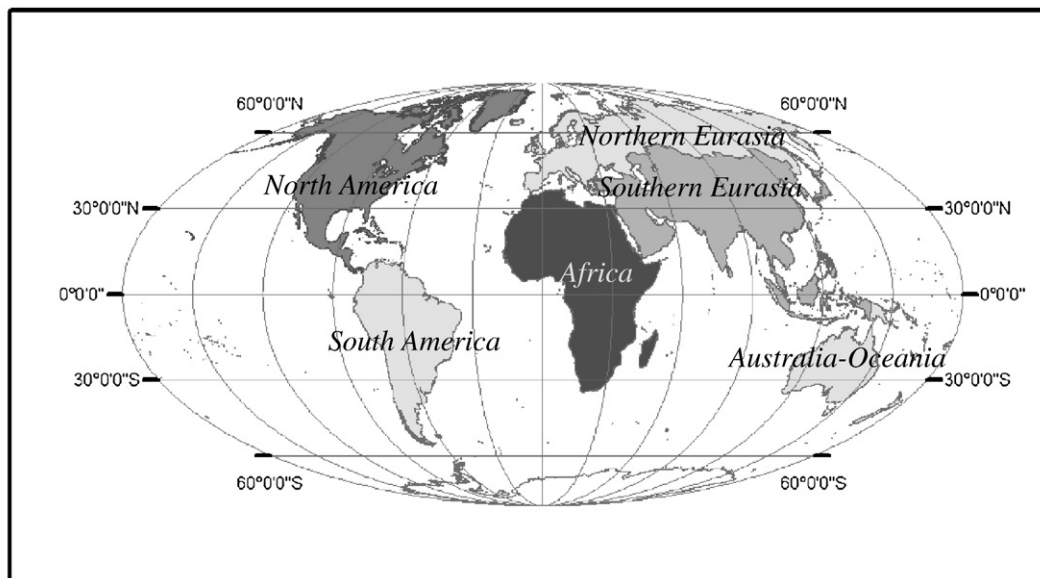


**Fig. 1.** Continental definition. All continents are considered together to derive the global results.

MODIS data (Giglio et al., 2006a). Although the global MODIS active fire calibration provided good agreement in some geographic regions it had and poor agreement in other regions and highlighted the complexity of the calibration task (Giglio et al., 2006a). Little research has been undertaken to examine the differences between active fire and burned area products generated by direct mapping. Limited comparison of the Collection 4 MODIS burned area and active fire products indicated several remote sensing, environmental, and fire behavior factors that may influence product differences, and, that in certain forested environments, counting active fire detections may provide greater total area burned estimates than generated by direct mapping (Roy et al., 2005a). In the Roy et al. (2005a) study, limited product comparisons were made temporally (~1 month) and spatially (~450 × 250 km) and the entire extent of the MODIS 1 km active fire and of the 500 m burned area product pixels was assumed to be burned. The MODIS burned area product labeled approximately three times a greater proportion of the landscape as burned than the active fire detection product in grassland and open woodland systems in Australia and Southern Africa. As only about 10% of the day and night MODIS active fire observations were labeled as cloud obscured it was concluded that this relative active fire under detection was due to the MODIS overpass occurring at times when the fires were not actively burning (Giglio, 2007) and/or to the active fires being insufficiently hot and/or large to be detected (Giglio et al., 2003; Giglio & Justice, 2003). Conversely, there was an observed under detection of the burned area product relative to the active fire product in forested regions of Brazil and of the Russian Federation. In these forested regions it was postulated that the active fire product may detect small active fires, if sufficiently hot, that were not detected in the burned area product if an insufficiently complete or large fraction of the MODIS 500 m pixel burned (Roy & Landmann, 2005). It was also suggested that under detection by the MODIS burned area product relative to the active fire product in these forested regions may have been due to obscuration of surface fires by overstorey vegetation, and/or because the active fire product overestimates the area burned where the majority of burned areas are smaller than 1 km pixels. This paper comprehensively documents these differences at global scale.

First the MODIS burned area algorithm and product are reviewed, then a statistical comparison of the Collection 5 MODIS burned area and active fire products is described with respect to global stratifications defined by percent tree cover and leaf area index ranges, then statistics of the annual and monthly total area burned defined by the

two MODIS fire products are reported globally and for each continent with respect to land cover classes, and then the product differences discussed in terms of factors concerned with remote sensing and environmental spatio-temporal fire characteristics.

## 2. Overview of the MODIS global burned area algorithm and product

Burned areas are characterized by deposits of charcoal and ash, removal of vegetation, and alteration of the vegetation structure (Pereira et al., 1997; Roy et al., 1999). The MODIS algorithm used to map burned areas takes advantage of these spectral, temporal, and structural changes using a change detection approach (Roy et al., 2005a). It detects the approximate date of burning at 500 m by locating the occurrence of

**Table 1**

Total number of 1 km active fires [ $\text{km}^2$ ] detected globally, July 2001 to June 2002, in each of the 12 MODIS UMD land cover classes

	Total active fires [ $\text{km}^2$ ] low-med-hi confidence	Total active fires [ $\text{km}^2$ ] only med-hi confidence	Decrease [%]
Evergreen needleleaf forest	2.71E+04	2.54E+04	6.45%
Deciduous needleleaf forest	9.43E+03	8.82E+03	6.45%
Evergreen broadleaf forest	1.71E+05	1.61E+05	6.09%
Mixed forests	5.09E+04	4.87E+04	4.28%
Closed shrublands	2.51E+04	2.41E+04	4.13%
Open shrublands	3.41E+05	3.27E+05	3.99%
Grasslands	2.11E+05	2.03E+05	3.84%
<b>All vegetation classes</b>	<b>2.90E+06</b>	<b>2.79E+06</b>	<b>3.80%</b>
Croplands	3.55E+05	3.43E+05	3.49%
Deciduous broadleaf forest	8.14E+04	7.86E+04	3.48%
Barren or sparsely vegetated	2.68E+04	2.58E+04	3.43%
Woody savannas	7.32E+05	7.07E+05	3.37%
Savannas	8.37E+05	8.10E+05	3.25%

The totals considering all active fire detections regardless of their confidence (high, medium and low confidence) and considering only high and medium confidence detections, and the percentage decrease between the two totals computed as (sum of low confidence detections/sum of all detections)\*100, are tabulated. The rows are ranked in descending order of percentage decrease.

rapid changes in daily surface reflectance time series data. The algorithm maps the spatial extent of recent fires and not of fires that occurred in previous seasons or years, and requires the consistently calibrated and processed MODIS data provided by the NASA MODIS land production system (Justice et al., 2002b; Masuoka et al., in press).

A bi-directional reflectance model-based change detection approach is applied independently to each gridded MODIS pixel. MODIS reflectances sensed within a temporal window of a fixed number of days are used to predict the reflectance on a subsequent day. Rather than attempting to minimize the directional information present in wide field-of-view satellite data by compositing, or by the use of spectral indices, this information is used to model the directional dependence of reflectance, commonly defined by the Bi-directional Reflectance Distribution Function (BRDF). This provides a semi-physically based method to predict change in reflectance from the previous state. A statistical measure is used to determine if the difference between BRDF model predicted and observed reflectance in the near and middle infrared bands indicate a significant change of interest. The statistical measure takes into account the error due to sensor calibration and atmospheric correction, the lack of ability of the BRDF model to fit the MODIS observations sensed within the temporal window, and the geometrical sampling quality of the observations. This approach is repeated independently for each pixel, moving through the reflectance time series in daily steps. A temporal constraint is used to differentiate between temporary changes, such as shadows, that are spectrally similar to more persistent fire induced changes. The identification of the date of burning is constrained by the frequency and occurrence of missing

observations and to reflect this, the algorithm is run to report the burn date with an 8 day precision. Further algorithm details and Equations are provided in Roy et al., 2005a.

The Collection 5 MODIS burned area product, like the other MODIS land products, will not be changed until a complete global reprocessing is undertaken as part of a future Collection 6. The Collection 5 product has a "provisional" status, designated by the MODIS science team to mean that the product quality is sufficient for use by the research community, but algorithm refinements may be underway to improve its performance (Justice et al., 2002b; Masuoka et al. in press). The MODIS burned area product is available to the user community ([WWW1](#)) and any changes to the MODIS burned area product generation algorithm and burned area product will not occur until Collection 6, which is not yet scheduled.

The MODIS burned area product is distributed as a monthly gridded 500 m product in Hierarchical Data Format (HDF). It is defined, like the other Collection 5 geolocated MODIS land products, in the Sinusoidal equal area projection in fixed earth-location tiles, each covering approximately  $1200 \times 1200$  km ( $10^\circ \times 10^\circ$  at the equator) (Wolfe et al., 1998). Three months of atmospherically and geometrically corrected, cloud-screened daily reflectance data (Vermote et al., 2002; Wolfe et al., 2002) are processed to generate each monthly product. Burning detected in the middle month plus and minus 8 days (the detection precision) is reported. The product includes descriptive metadata and several 500 m data layers. The data layers define for each gridded land pixel: the approximate Julian day (1–366) of burning or a code indicating unburned, no burning detected but snow detected, no burning detected but water detected, or insufficient

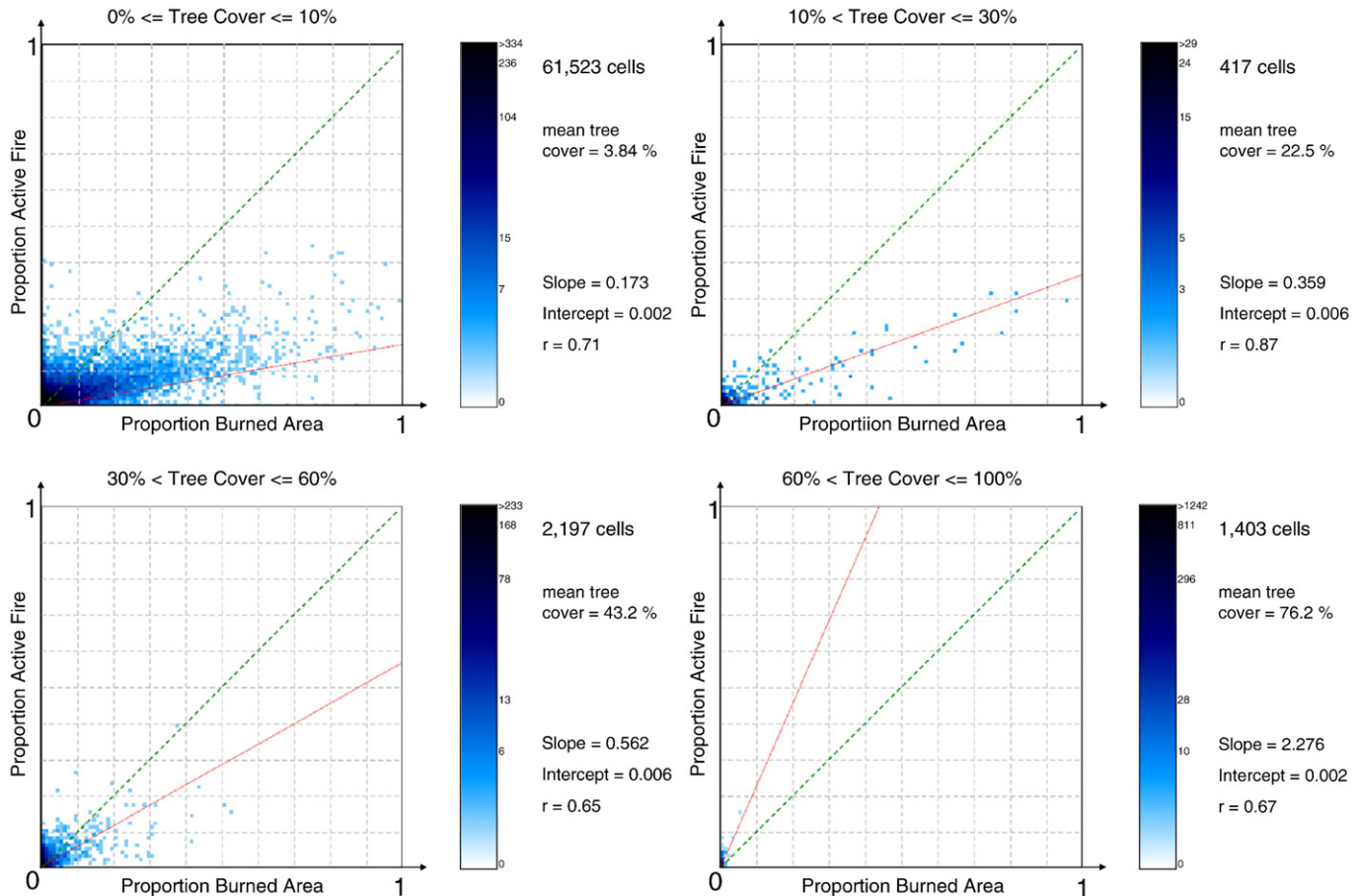


**Fig. 2.** Scatter plots of the monthly proportions of  $40 \times 40$  km cells labeled as burned by the 1 km active fire detections plotted against the proportion labeled as burned by the 500 m burned area product, for four percent tree cover class ranges, globally, all 12 months July 2001 to June 2002. Only cells with at least 90% of their area meeting these percent tree cover range criteria and containing some proportion burned in either the active fire or the monthly burned area products are plotted. The Theil-Sen regression line is plotted in red; the white-blue logarithmic color scale illustrates the frequency of cells having the same specific x and y axis proportion values. These data are generated from the monthly 500 m MODIS burned area and the monthly 1 km day and night active fire (medium and high confidence detections) composites described in the text.

number of observations to make a detection decision (usually due to cloud or missing data); the detection confidence (1 – most confident to 4 – least confident); information describing the two largest numbers of consecutive missing/cloudy days (if any) in the month plus and minus 8 days; and ancillary quality information describing the land and atmospheric properties and processing path information.

### 3. Study area and period

Annual and monthly analysis for the six continental areas illustrated in Fig. 1 and globally are reported. Natural and anthropogenic fires occur on all continents except Antarctica which is not considered. This continental definition is not a geographic stratification of fire regimes, but is used to provide a reduced number of geographically contiguous regions for reporting purposes. The continents are defined using the continental vectors of the National Imagery and Mapping Agency (NIMA) Digital Chart of the World (WW2). All the territories of a country are assigned to the same continent, for example, all the territories of the Russian Federation are together with Europe (Northern Eurasia). Analysis with respect to different land cover types are also reported to provide more insights into the patterns of burning.

The first available (at the time of writing) consecutive 12 months of global MODIS burned area product data of consistent quality, July 2001 to June 2002, are analyzed on a monthly and annual basis. Based on global fire assessments in the peer reviewed literature (Giglio et al., 2006b; Van Der Werf et al., 2006; Tansey et al., 2008), this study period can be considered as being representative of recent global fire distributions, without extreme fire events such as those associated with

the Indonesia fires of 1997–1998, the 2004 fires in Siberia, or the Mediterranean fires in 2003 and 2007. We recognize the limitation of a single year analysis as there is considerable inter-annual variability in the distribution and extent of fires (Giglio et al., 2006b); for example, certain regions, such as boreal forests, may burn only once every decade to tens of decades, whereas grassland systems may burn every year (Kasischke et al., 1995; Van Wilgen et al., 2004; Bond et al., 2005). We assume however that the continental definition is sufficiently large to capture inter-annual fire variability that may be missed at smaller spatial sampling scales. For example, forest stand replacing fires may occur only every several hundred years in a specific locality but at several locations in the same year at the continental scale.

### 4. Data and preprocessing

The most recently generated MODIS product collections are used in this analysis i.e., Collection 5 500 m monthly burned area, 1 km daily active fire and 1 km 8-day leaf area index products; Collection 4 1 km annual land cover and 500 m annual percent tree products. Some processing, described below, was undertaken to produce comparable monthly data sets.

The MODIS burned area product (MCD45A1) is distributed as a monthly 500 m product reporting the approximate day of burning between 8 days before and after the calendar month period. As a consequence, there is always a 16 day overlap period between consecutive months in which the same burn can be detected on the same day, or, because of algorithm sensitivity to the frequency and occurrence of missing observations, on slightly different days. For this study we generated a temporally filtered version of the monthly

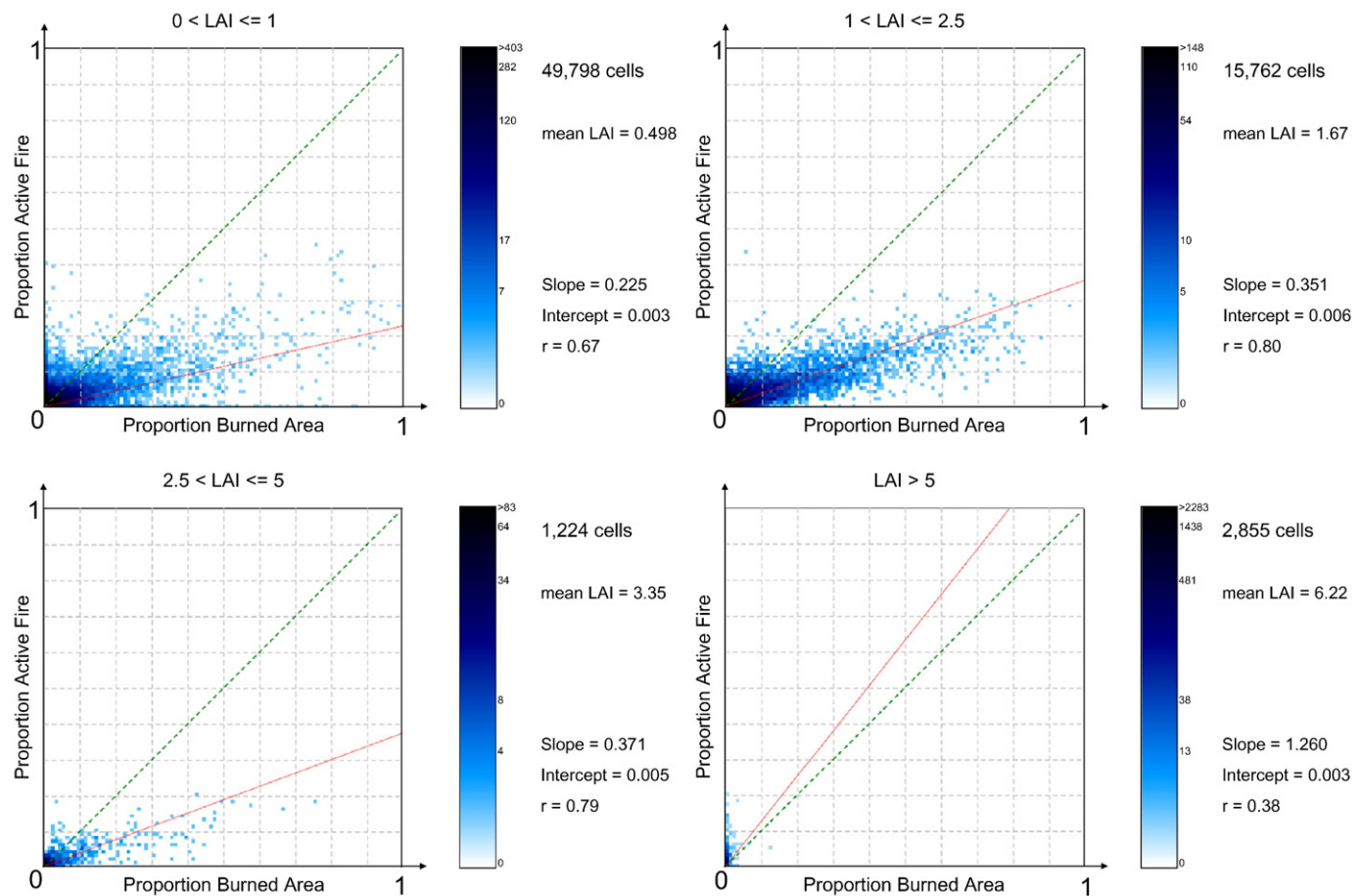


**Fig. 3.** Scatter plots of the monthly proportions of 40×40 km cells labeled as burned by the 1 km active fire detections plotted against the proportion labeled as burned by the 500 m burned area product, for four leaf area index (LAI) ranges, globally, all 12 months July 2001 to June 2002. Only cells with at least 90% of their area meeting these LAI range criteria and containing some proportion burned in either the active fire or the monthly burned area products are plotted. Other details as Fig. 2.

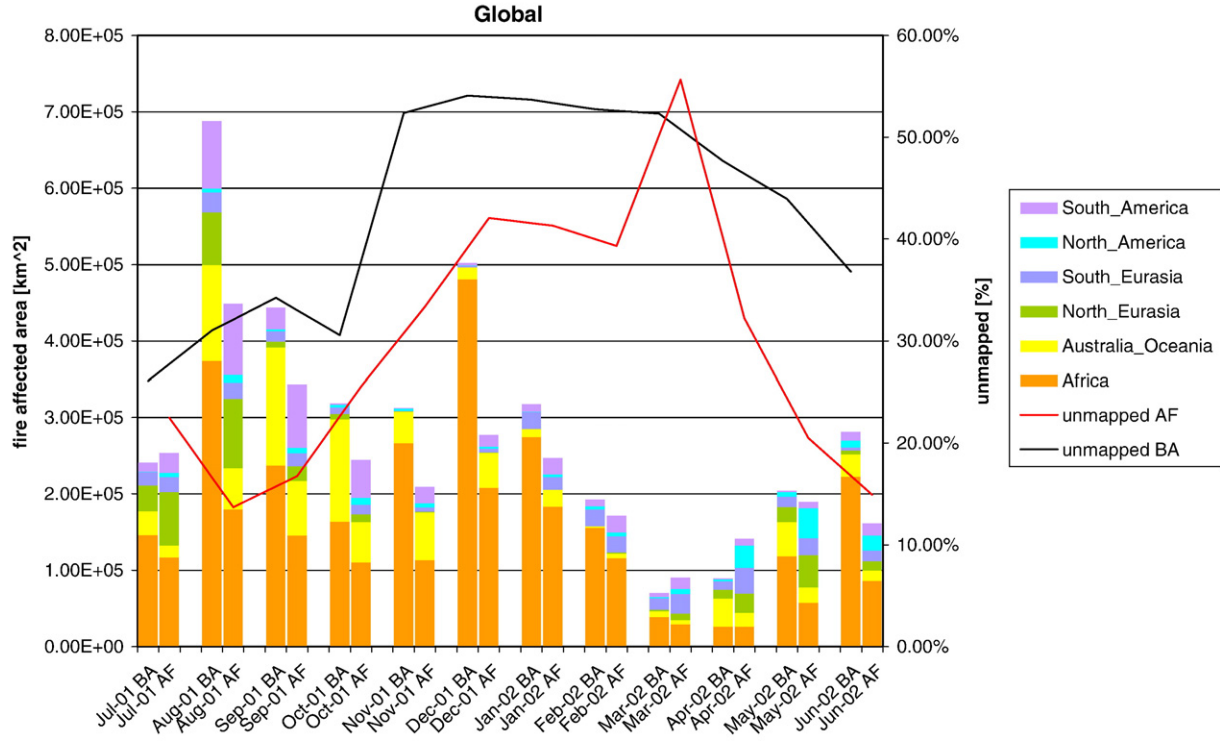


**Fig. 4.** Monthly histograms of fire affected area by continent (Fig. 1) detected by the MODIS burned area (BA) product (left bar) and the MODIS active fire (AF) product (right bar). The black lines show the global percentage of unmapped pixels in the monthly burned area product; the red lines show the global average of the percentage of unmapped days according to the active fire product; see text for further details.

product that uses the MCD45A1 quality and processing path information to allocate burns in the overlap period to the most likely calendar month in order to preclude potential double-counting of burned areas when consecutive months are considered.

The MODIS active fire product detects fires in 1 km pixels that are burning at the time of overpass under relatively cloud-free conditions (Giglio et al., 2003; Giglio, 2007). The 1 km daily MODIS active fire product (MOD14A1) reports the occurrence of active fires detected over a 24 hour period as sampled during the 4 Terra and Aqua overpasses and the detection confidence (high, medium or low) (Giglio et al., 2003). If no detections occurred then the surface state (land, water, unknown, snow or cloud) is recorded. In this study, low confidence active fire detections were not considered in order to reduce potential active fire commission errors. To investigate the impact of this, the total number of 1 km active fires detected globally was quantified considering all active fire detections regardless of their confidence (high, medium and low confidence) and considering only the high and medium confidence detections, further, to investigate any land cover dependency to the incidence of low confidence active fires, the comparison was considered with respect to each of the 12 MODIS UMD land cover classes (Table 1). Globally, for the 12 months con-

sidered, there were on average 3.8% fewer active fire detections when low confidence detections were excluded. The occurrence of low confidence detections was greatest in the forest classes, with at most 6.45% fewer detections for the evergreen needle leaf forest class, and the smallest difference for the savanna class (3.25% less detections when low confidence active fire detections were not considered). This underscores earlier commentary that active fire detections may be less reliable in forested regions, and is discussed in Section 7. The high and medium confidence 1 km active fire detections were aggregated temporally into monthly composites that define the location of 1 km pixels with an active fire detection in that month, or if no detection, then the percentage of the days with cloud or snow or missing data, and a code indicating if the pixel was water or unknown surface status.

The MODIS percent tree product (MOD44B) reports the percent tree cover mapped at 500 m using a supervised regression tree applied to a year of MODIS data (Hansen et al., 2003). In the following analyses, the monthly 2001 and 2002 fire products were compared with the 2000 and 2001 percent tree cover products respectively to ensure that percent tree cover information derived before fire occurrence was considered.

The MODIS leaf area index (MOD15A2) product reports the green leaf area index (LAI), defined as the one-sided green leaf area per unit ground

**Table 2**  
Total burned area defined by the MODIS burned area product (MCD45) and by the active fire product (medium and high confidence detections) (MOD14), globally, July 2001 to June 2002, in each of the six continents (Fig.1)

Continent	Burned area (MCD45) [km <sup>2</sup> ]	Active fires (MOD14) [km <sup>2</sup> ]	Area [km <sup>2</sup> ]	Average annual unmapped area (MCD45)	Average annual unmapped area (MOD14)	Percentage of MCD45 burned area mapped in this continent	Percentage of MOD14 fire affected area mapped in this continent
Africa	2.50E+06	1.37E+06	2.97E+07	19.20%	15.46%	68.41%	49.40%
Australia-Oceania	6.32E+05	3.87E+05	8.48E+06	10.35%	13.06%	17.26%	13.94%
Northern Eurasia	1.56E+05	2.82E+05	2.22E+07	68.08%	50.43%	4.26%	10.16%
Southern Eurasia	1.56E+05	2.14E+05	3.08E+07	45.38%	25.31%	4.27%	7.70%
North America	4.01E+04	1.43E+05	2.28E+07	53.61%	44.71%	1.10%	5.17%
South America	1.72E+05	3.79E+05	1.75E+07	49.13%	24.74%	4.70%	13.64%
TOTAL	3.66E+06	2.78E+06	1.31E+08	42.96%	29.82%	100%	100%

The global area of each continent and the annual average percentage of this area that was unmapped are also shown.

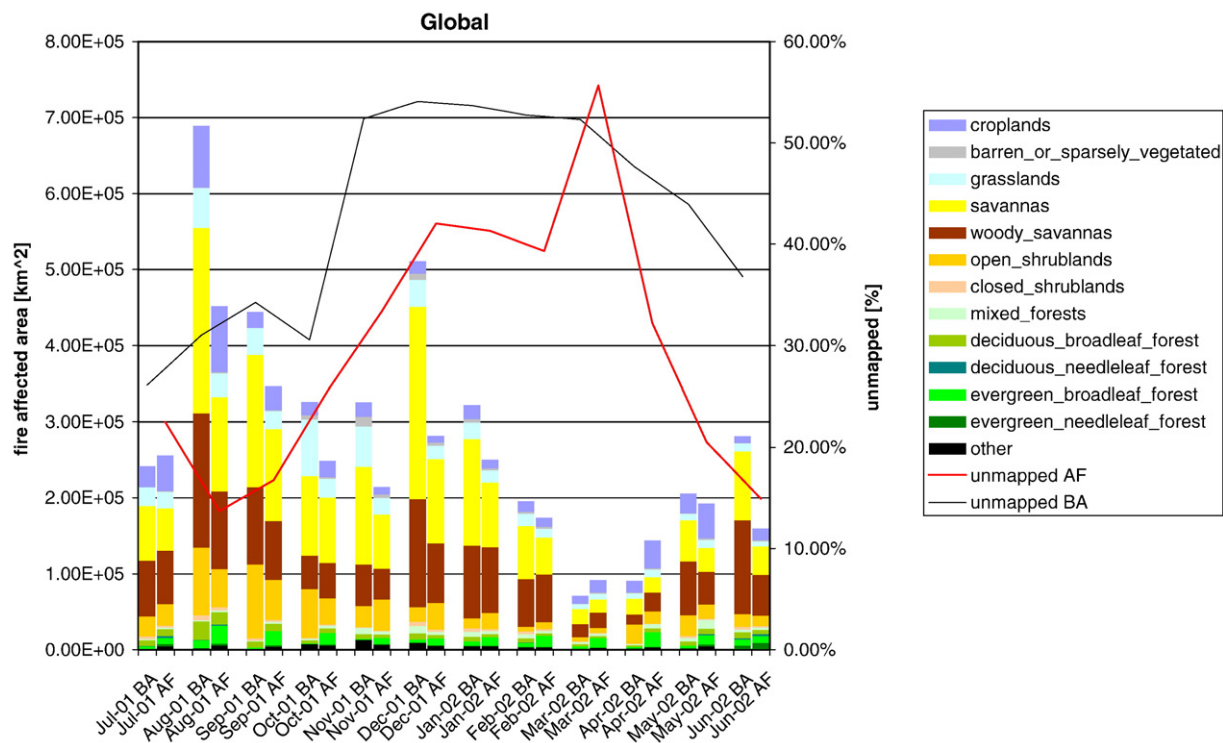


**Fig. 5.** Monthly histograms of fire affected area detected globally by the MODIS burned area (BA) product (left bar) and the MODIS active fire (AF) product (right bar) for different MODIS vegetation classes. The black lines show the global percentage of unmapped pixels in the monthly burned area product; the red lines show the global average of the percentage of unmapped days according to the active fire product; see text for further details.

area in broadleaf canopies and as half the total needle surface area per unit ground area in coniferous canopies, at 1 km every 8 days (Myndeni et al., 2002). These data were composited into monthly 1 km data sets by selecting the maximum good quality LAI value over each month (Myndeni et al., 2007). In the following analyses, monthly fire products were compared with the monthly LAI composite from the previous month to ensure that only pre-fire LAI information was considered.

The MODIS land cover product (MOD12Q1) defines the annual 1 km land cover with respect to a number of classification schemes (Friedl et al., 2002). The land cover product produced for 2001 and the

University of Maryland (UMD) classification scheme (Hansen et al., 2000) were used. The UMD classification scheme was included here to ensure compatibility with previous research reporting burned area and emissions at global and continental scale (Tansey et al., 2004; Korontzi et al., 2006; Michel et al., 2005).

## 5. Methodology

The MODIS 1 km active fire and the MODIS 500 m burned area products are compared in a globally stratified manner, first by

**Table 3**

Total burned area defined by the MODIS burned area product (MCD45) and by the active fire product (medium and high confidence detections) (MOD14), globally, July 2001 to June 2002, in each of the MODIS land cover classes (class "Other" includes urban, inland water bodies and unclassified)

Vegetation class	Burned area (MCD45) [km <sup>2</sup> ]	Active fires (MOD14) [km <sup>2</sup> ]	Area [km <sup>2</sup> ]	Average unmapped area (MCD45)	Average unmapped area (MOD14)	Percentage of MCD45 burned area mapped in this class	Percentage of MOD14 fire affected area mapped in this class
Evergreen needleleaf forest	1.18E+04	2.54E+04	5.67E+06	73.81%	65.72%	0.32%	0.91%
Evergreen broadleaf forest	4.84E+04	1.61E+05	1.46E+07	70.00%	46.04%	1.32%	5.80%
Deciduous needleleaf forest	2.50E+03	8.82E+03	9.59E+05	76.79%	30.22%	0.07%	0.32%
Deciduous broadleaf forest	8.87E+04	7.86E+04	2.33E+06	34.41%	57.68%	2.42%	2.83%
Mixed forests	4.87E+04	4.87E+04	6.82E+06	63.13%	24.26%	1.33%	1.75%
Closed shrublands	3.67E+04	2.14E+04	8.00E+05	26.43%	38.46%	1.00%	0.87%
Open shrublands	4.19E+05	3.27E+05	2.66E+07	39.97%	17.31%	11.43%	11.78%
Woody savannas	9.76E+05	7.07E+05	1.10E+07	46.49%	35.30%	26.65%	25.45%
Savannas	1.37E+06	8.10E+05	1.02E+07	32.30%	30.24%	37.40%	29.15%
Grasslands	3.46E+05	2.03E+05	1.35E+07	45.41%	20.10%	9.46%	7.30%
Croplands	2.76E+05	3.43E+05	1.61E+07	44.20%	26.02%	7.53%	12.35%
Barren or sparsely vegetated	3.71E+04	2.58E+04	2.21E+07	15.51%	23.86%	1.01%	0.93%
Other	7.60E+03	2.68E+04	3.63E+06	67.46%	56.81	0.23%	0.97
TOTAL	3.66E+06	2.78E+06	1.31E+08	42.96%	29.82%	100%	100%

The global area of each vegetation class and the annual average percentage of this area that was unmapped are also shown.

comparison of the proportions burned in fixed geolocated 40 km × 40 km grid cells overlaid on each product, and second by comparison of the total area burned for the six continents and globally. The former comparison is required to quantify the degree of product spatio-temporal correspondence; especially as continental burned area statistics may be similar for the two products but fire detected at different locations. In this analysis, as in Roy et al. (2005a),

all of the 500 m burned area product pixels, and all of the 1 km active fire product pixels are assumed to be burned respectively. We recognize that this is arbitrary, but assuming some other sub-pixel fraction would also be arbitrary, and in all cases, at the scale of this study, may cause systematic biases in certain environments in a manner that is dependent on the spatio-temporal characteristics of fire. This is discussed in more detail in Section 7.

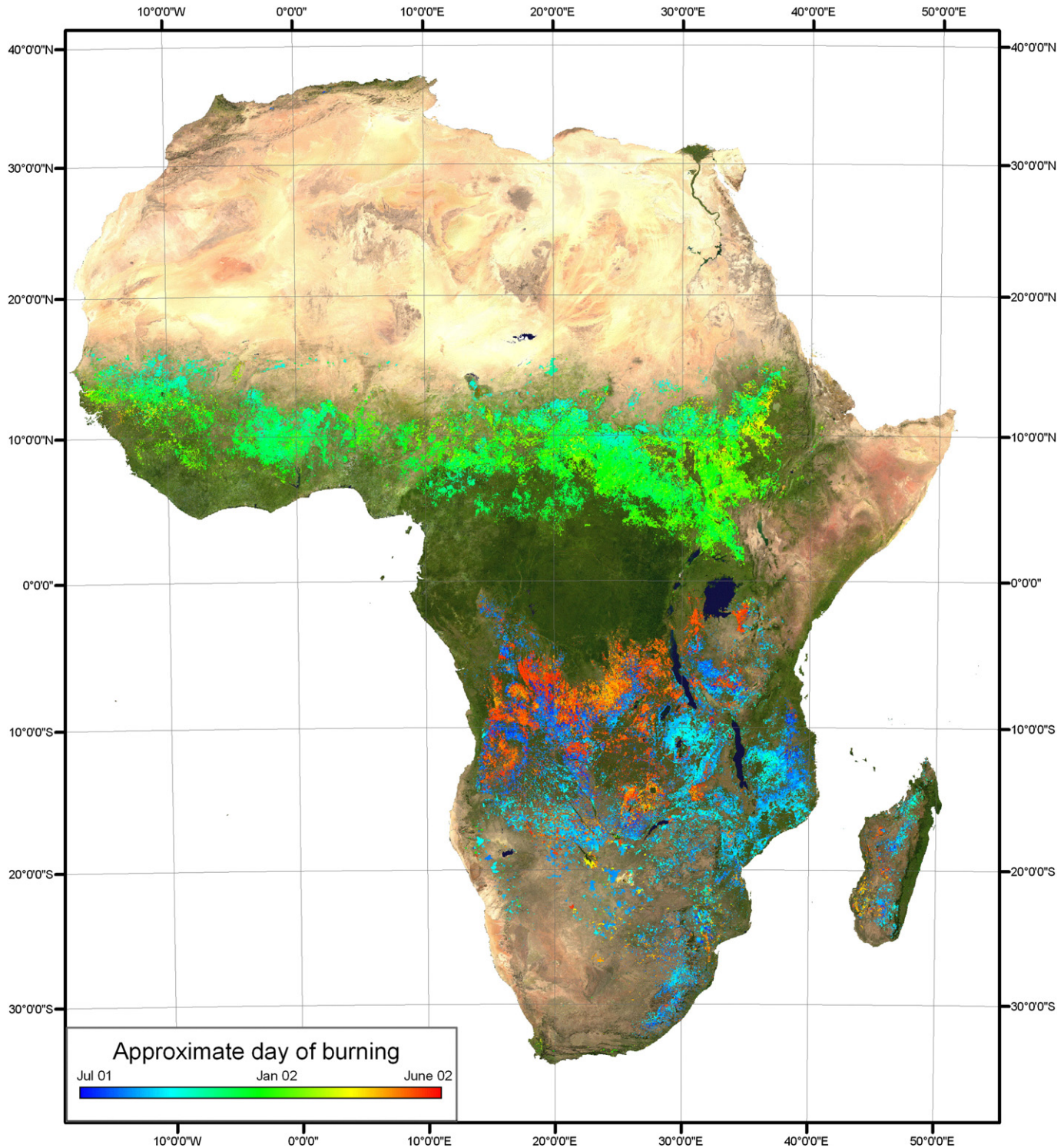


**Fig. 6.** Africa subset of the global MODIS burned area product, for the July 2001–June 2002 period. Burned areas are displayed in a rainbow color scale according to the detection date, from blue (July 2001) to red (June 2002). To provide geographic context, the burned areas are superimposed on the NASA Blue Marble true color MODIS surface reflectance composite. Projection: Albers Equal Area Conic.

### 5.1. Product comparison – proportions burned in fixed geolocated grid cells stratified by percent tree cover and by leaf area index

The MODIS active fire and burned area products are compared in a spatio-temporally explicit manner with respect to  $40 \times 40$  km grid cells. Scatter plots of the proportions of the cells labeled as burned by the medium and high confidence 1 km active fire detections plotted against the proportions labeled as burned by the 500 m burned area product, are generated for the entire study period globally. Proportions are defined as the  $40 \times 40$  km grid cell area divided by the sum of the labeled product pixel areas that fall within the cell. The analysis is undertaken for different percent tree cover and leaf area index (LAI) strata to quantify more comprehensively the grassland and forest Collection 4 MODIS fire product differences reported in Roy et al. (2005a). The scatterplots are defined for four ranges of MODIS percent tree cover, following the IGBP tree cover quantization (Rasool, 1992): percent tree 0% to  $\leq 10\%$ ,  $> 10\%$  to  $\leq 30\%$ ,  $> 30\%$  to  $\leq 60\%$  and  $> 60\%$  to  $\leq 100\%$ ; and defined for four ranges of MODIS LAI to capture low to high LAI variation: 0 to  $\leq 1$ ,  $> 1$  to  $\leq 2.5$ ,  $> 2.5$  to  $\leq 5$ ,  $> 5$  (Myneni et al., 2002). Only cells with at least 90% of their area meeting these stratification criteria and containing some proportion burned in either the monthly active fire or the monthly burned area products are plotted. The 12 months are independently compared and the scatterplots generated for all 12 months combined.

Linear regression results are derived from the scatterplots to quantify the observed relationships, and the correlation between predicted values and observed values are shown as an indicator of the goodness of fit. As there is no guarantee that the active fire and burned area proportions are error free, the Theil-Sen regression estimator is used (Theil, 1950; Sen, 1968). The Theil-Sen estimator is non-parametric, robust to outliers, and unlike ordinary least squares regression estimators makes only weak assumptions about the response and predictor errors (Curran & Hay, 1986; Fernandes & Leblanc, 2005). A 40 km grid cell dimension was selected to keep the

total number of cells at a computable level (less than 64,000) as the Theil-Sen regression operation rapidly becomes computationally expensive as the number of measurements increases.

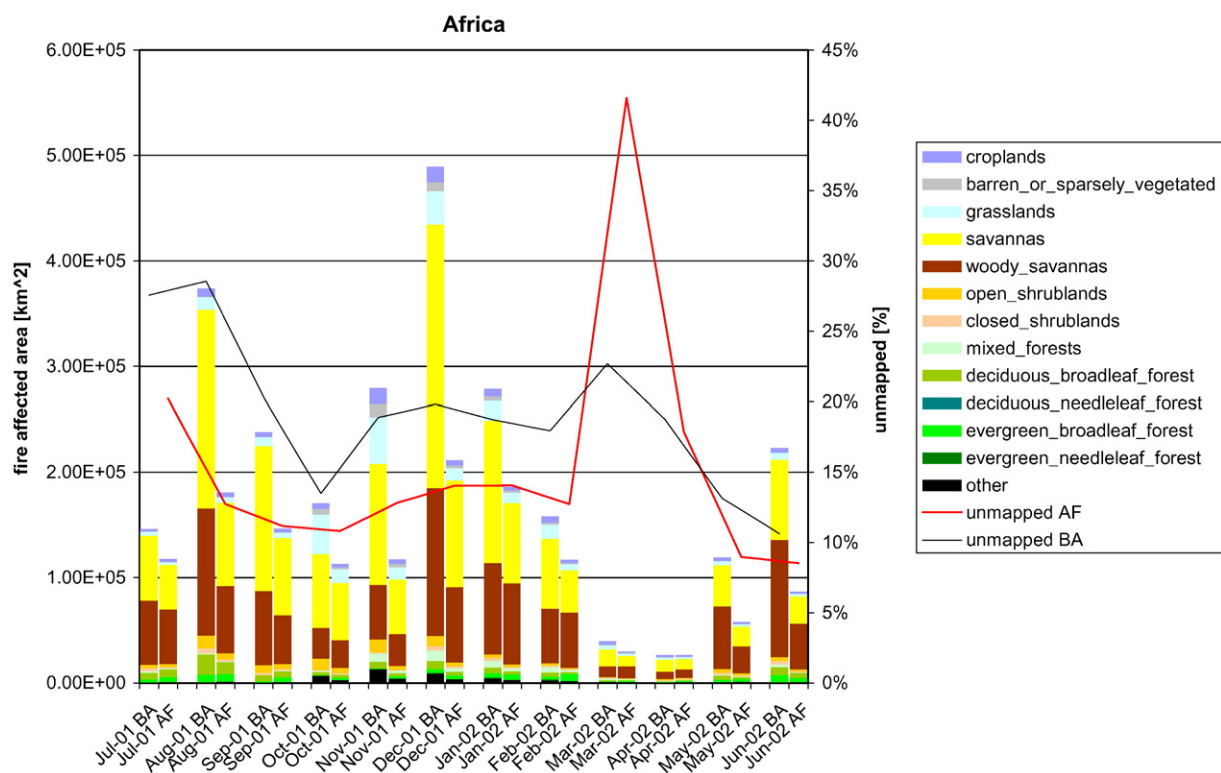
### 5.2. Product comparison – total area burned reporting

Statistics of the annual and monthly total area burned defined by the two MODIS fire products are reported with respect to the continental definitions (Fig. 1) and the MODIS UMD land cover product classes. Summary area burned statistics may be biased if unmapped pixels are not taken into account in the reporting. Unmapped MODIS active fire product pixels occur due to cloud or snow, water and unknown land surface status, and missing data caused by instrument or data processing failures (Gigli et al., 2003; Roy et al., 2002b). Unmapped MODIS burned area product pixels occur when insufficient reflectance time series data are available to invert the BRDF model, predominantly due to cloud or missing data (Roy et al., 2006). In this study, the unmapped areas are reported for both fire products in addition to the total area burned. To improve reporting compatibility between these products, the burned area product pixels labeled as no burning detected, but snow or water detected, are considered as unmapped.

## 6. Product comparison results

### 6.1. Product comparison – proportions burned in fixed geolocated grid cells stratified by percent tree cover and by leaf area index

Figs. 2 and 3 show scatter plots of the monthly proportions of  $40 \times 40$  km cells labeled as burned by the medium and high confidence 1 km active fire detections, plotted against the proportion labeled as burned by the 500 m burned area product, globally for the 12 month study period. Because of the large number of cells considered, a coloring scheme is used to illustrate the frequency of cells having the



same x and y axis proportion values. Fig. 2 shows scatterplots defined for four ranges of MODIS percent tree cover, and Fig. 3 shows scatterplots defined for four ranges of MODIS leaf area index (LAI).

Figs. 2 and 3 show a clear pattern. For low percent tree cover and LAI, the MODIS burned area product defines a greater proportion of the landscape as burned than the active fire product, but with increasing tree cover and LAI the MODIS active fire product defines a relatively greater proportion. In all plots the Theil-Sen regression line passes nearly through the origin (the maximum intercept values is 0.002) and the slopes of the regression lines increase with increasing tree cover and LAI. For percent tree cover ranges 0% to  $\leq 10\%$ ,  $>10\%$  to  $\leq 30\%$ ,  $>30\%$  to  $\leq 60\%$ , and  $>60\%$  to  $\leq 100\%$ , the slope increases from 0.17, 0.36, 0.56 to 2.77 respectively; i.e. for low percent tree covers ( $\leq 10\%$ ) the active fire product captures less than a fifth (0.17) of the area burned detected by the burned area product, but at high tree cover ( $>60\%$ ) it captures more than twice (2.28) the proportion. For all four percent tree cover ranges the correlation ( $r$ ) between the predicted and observed values indicates reasonable fits (the lowest  $r$  value is 0.56, the highest 0.87). The Fig. 3 results show the same pattern but less difference between the two products as a function of LAI; for LAI

ranges 0 to  $\leq 1$ ,  $>1$  to  $\leq 2.5$ ,  $>2.5$  to  $\leq 5$ , and  $>5$ , the slope increases from 0.22, 0.35, 0.37, 1.26 respectively, and the  $r$  values indicate reasonable fits ( $r > 0.67$ ) except for the LAI  $> 5$  range where  $r = 0.38$ . These results confirm, at the global scale, the findings of the limited MODIS active fire and burned area comparisons described by Roy et al., 2005a, and are discussed in more detail in Section 7.

## 6.2. Product comparison – total area burned reporting

### 6.2.1. Global results

Fig. 4 shows monthly histograms of the burning activity for the six continents and Table 2 summarizes these statistics. For each month the total burned area defined by the monthly 500 m MODIS burned area product and by the monthly 1 km MODIS day and night active fire composite is reported. All of the 500 m and all of the 1 km burned area and active fire product pixels are assumed to be burned respectively. Unlike the Figs. 2 and 3 scatterplots, the areas labeled as burned by these products may have occurred at different locations. Black lines show the percentage of unmapped pixels in the monthly burned area product, and red lines show the average of the percentage of the days

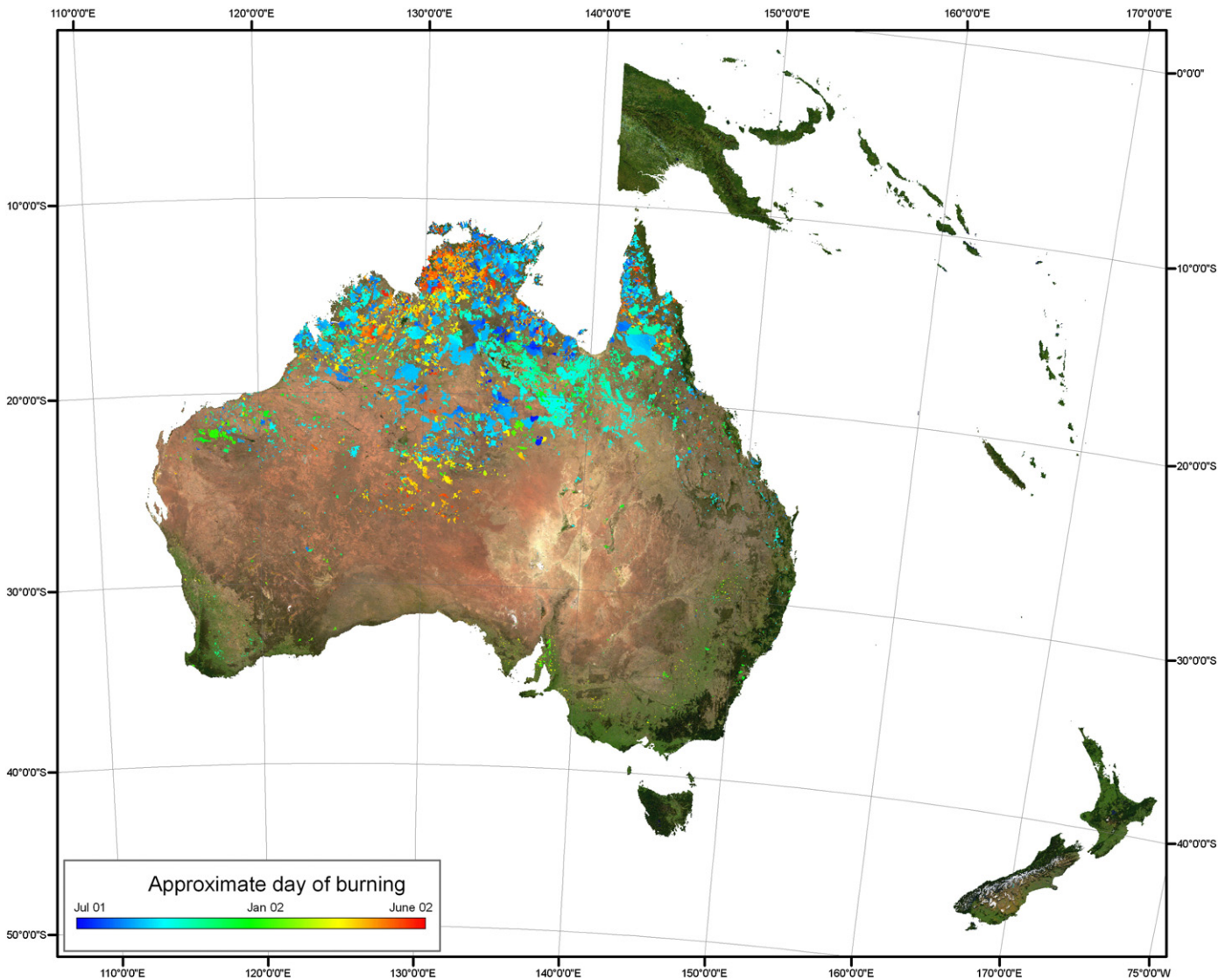


**Fig. 8.** Australia and Oceania subset of the global MODIS burned area product, for the July 2001–June 2002 period. Burned areas are displayed in a rainbow color scale according to the detection date, from blue (July 2001) to red (June 2002). To provide geographic context, the burned areas are superimposed on the NASA Blue Marble true color MODIS surface reflectance composite. Projection: Albers Equal Area Conic.

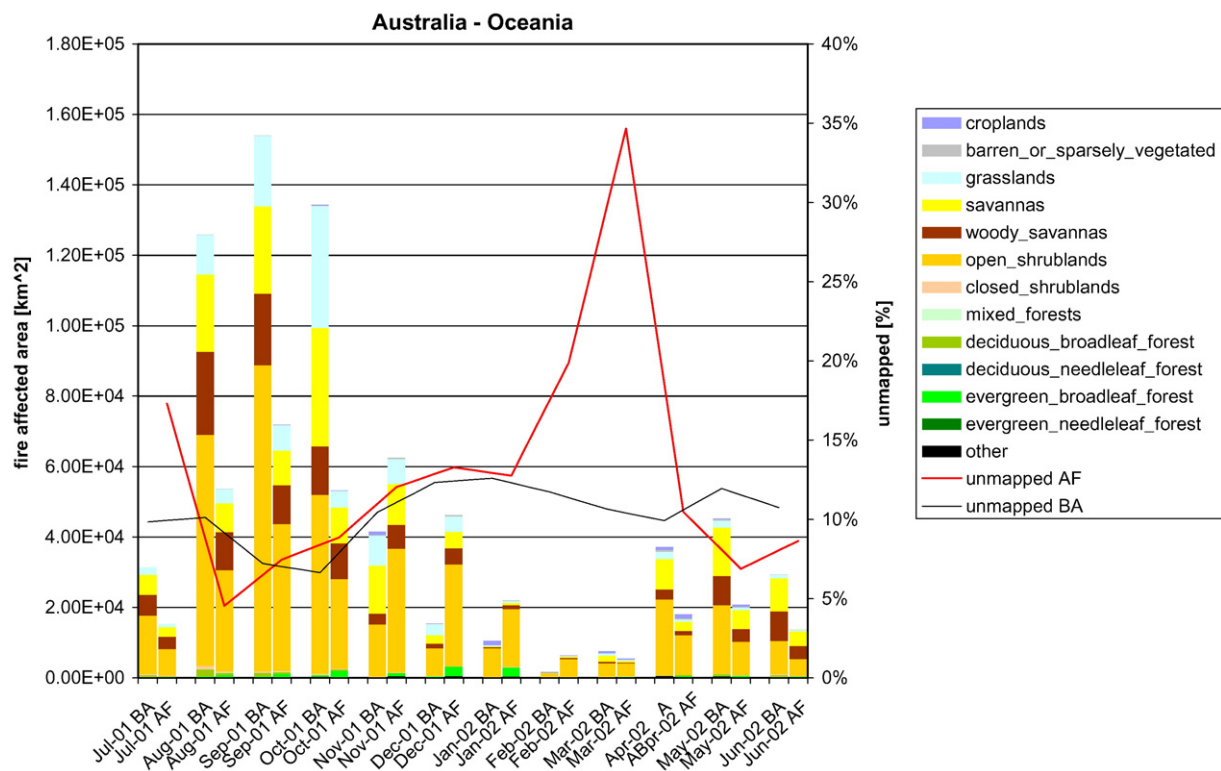


**Fig. 9.** Monthly histograms of fire affected area in Australia and Oceania detected by the MODIS burned area (BA) product (left bar) and the MODIS active fire (AF) product (right bar) for different MODIS vegetation classes. The black lines show, for Australia and Oceania, the percentage of unmapped pixels in the monthly burned area product and the red lines show the average of the percentage of unmapped days according to the active fire product.

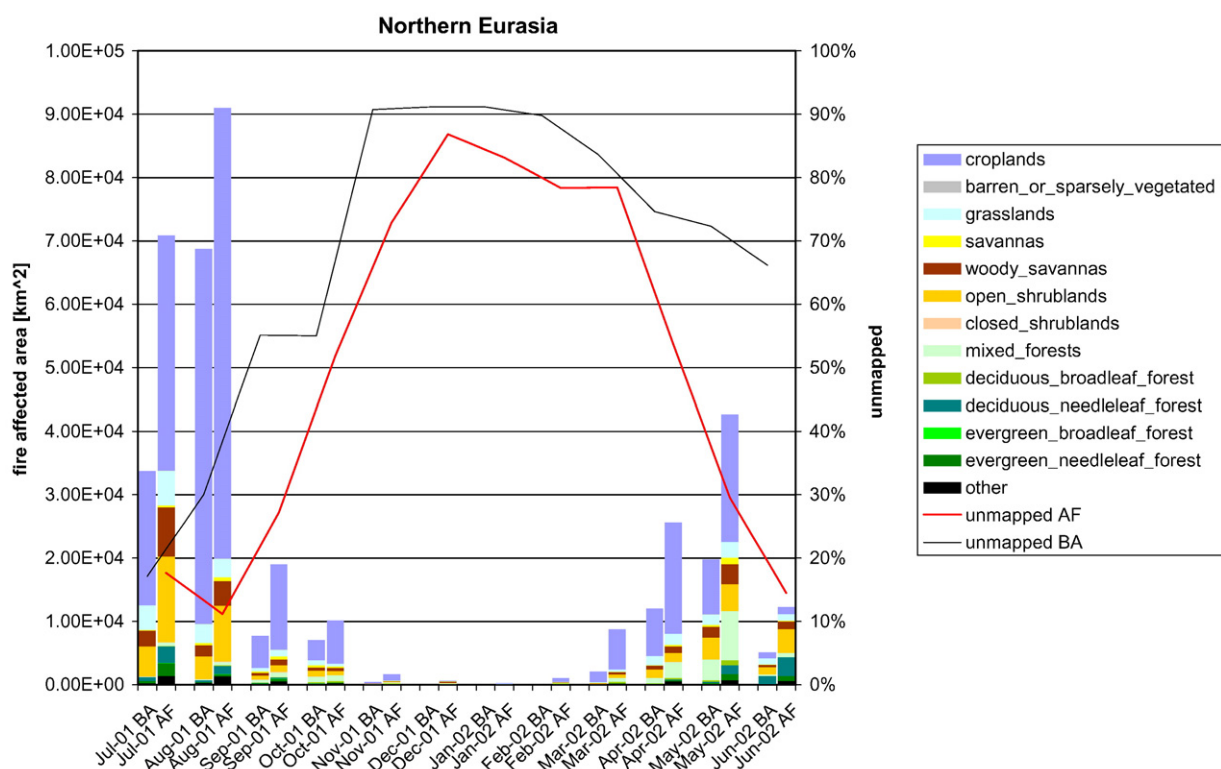


**Fig. 10.** Monthly histograms of fire affected area in Northern Eurasia detected by the MODIS burned area (BA) product (left bar) and the MODIS active fire (AF) product (right bar) for different MODIS vegetation classes. The black lines show, for Northern Eurasia, the percentage of unmapped pixels in the monthly burned area product and the red lines show, for Africa, the average of the percentage of unmapped days according to the active fire product.

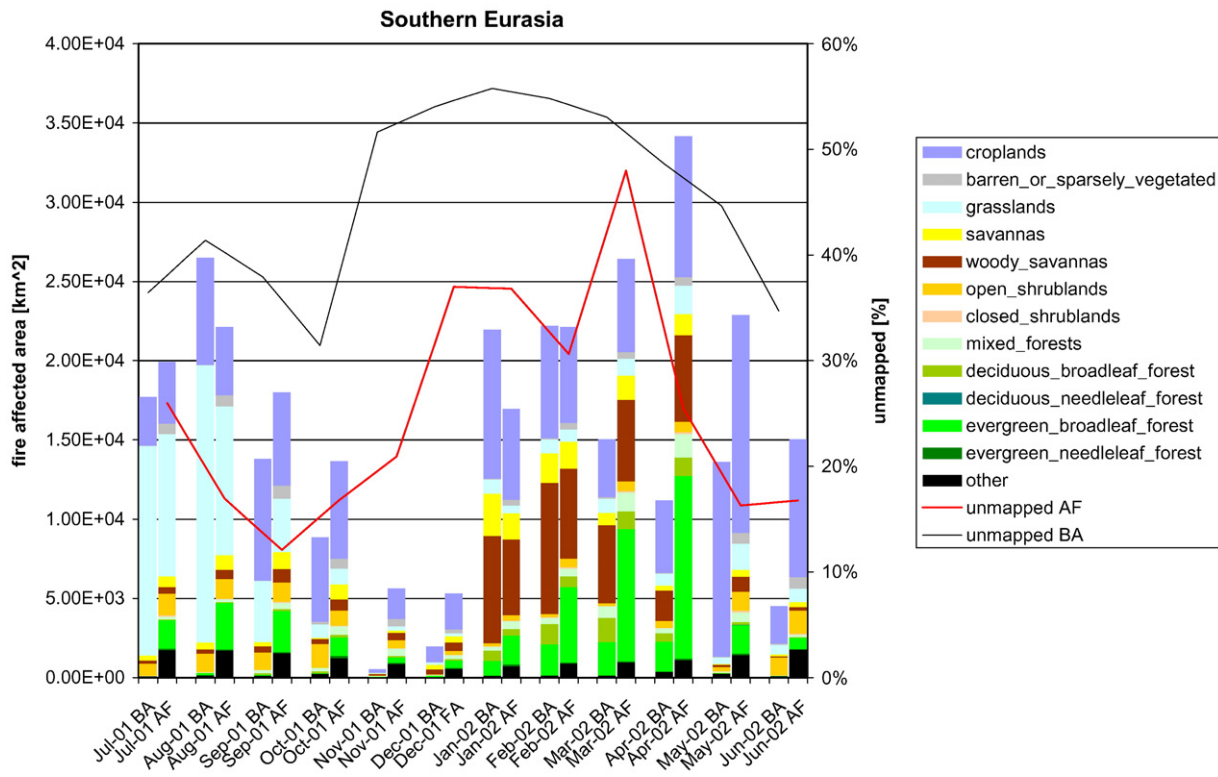


**Fig. 11.** Monthly histograms of fire affected area in Southern Eurasia detected by the MODIS burned area (BA) product (left bar) and the MODIS active fire (AF) product (right bar) for different MODIS vegetation classes. The black lines show, for Southern Eurasia, the percentage of unmapped pixels in the monthly burned area product and the red lines show, for Africa, the average of the percentage of unmapped days according to the active fire product.

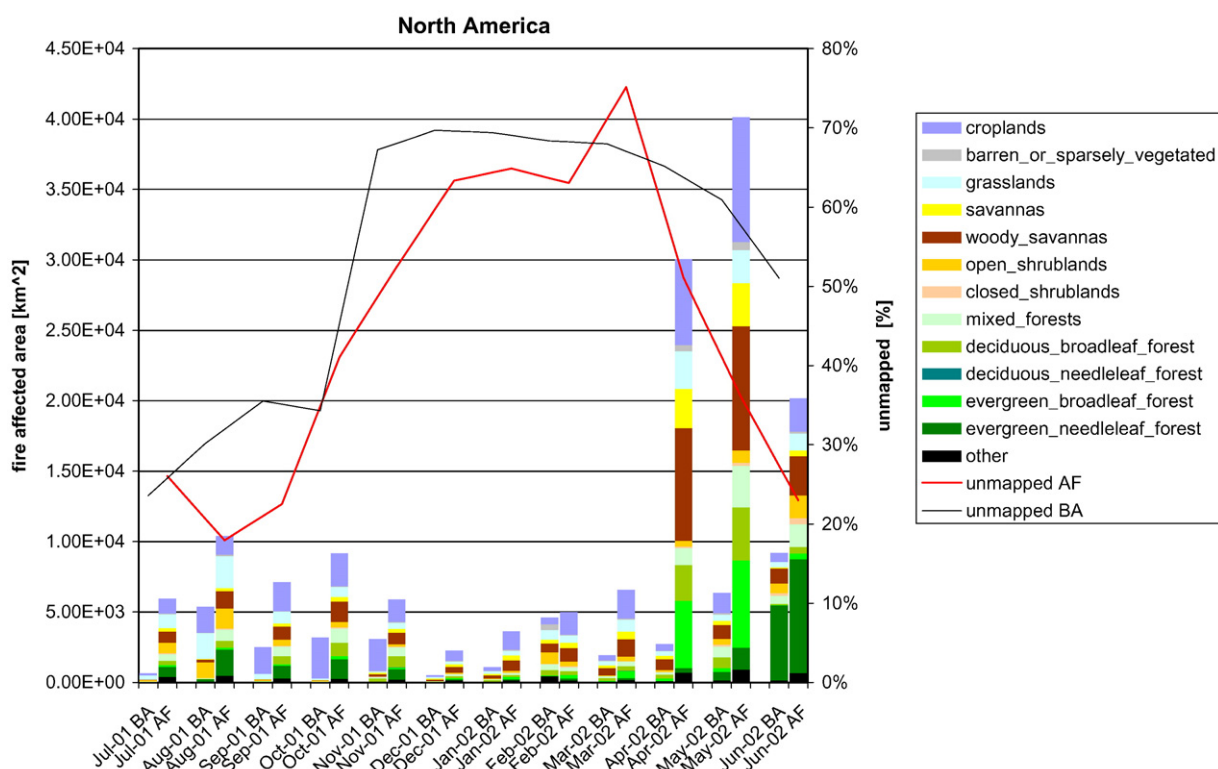


**Fig. 12.** Monthly histograms of fire affected area in North America detected by the MODIS burned area (BA) product (left bar) and the MODIS active fire (AF) product (right bar) for different MODIS vegetation classes. The black lines show, for North America, the percentage of unmapped pixels in the monthly burned area product and the red lines show, for Africa, the average of the percentage of unmapped days according to the active fire product.

unmapped by the active fire product. The anomalously high percentage of unmapped pixels March 2002 is due to eight consecutive days of missing data caused by a sensor failure.

Globally the total area burned labeled by the MODIS burned area product is  $3.66 \times 10^6 \text{ km}^2$  for July 2001 to June 2002 (Table 2), while the active fire product detected for the same period a total of  $2.78 \times 10^6 \text{ km}^2$ , i.e., about 24% less than the area labeled by the burned area product (Table 2). Africa and Australia-Oceania are by far the two

continents most affected by fire, with respectively 68% and 17% of the total burned area (Table 2). The remaining continents are responsible for only 14% of the area burned, despite representing about 70% of the land area considered in this study (Antarctica is not considered).

Burned area statistics are often reported over calendar years (January to December) which, combined with inter-annual fire variability, precludes direct comparison of the results reported here with other studies. Despite this, the total area burned of  $3.66 \times 10^6 \text{ km}^2$

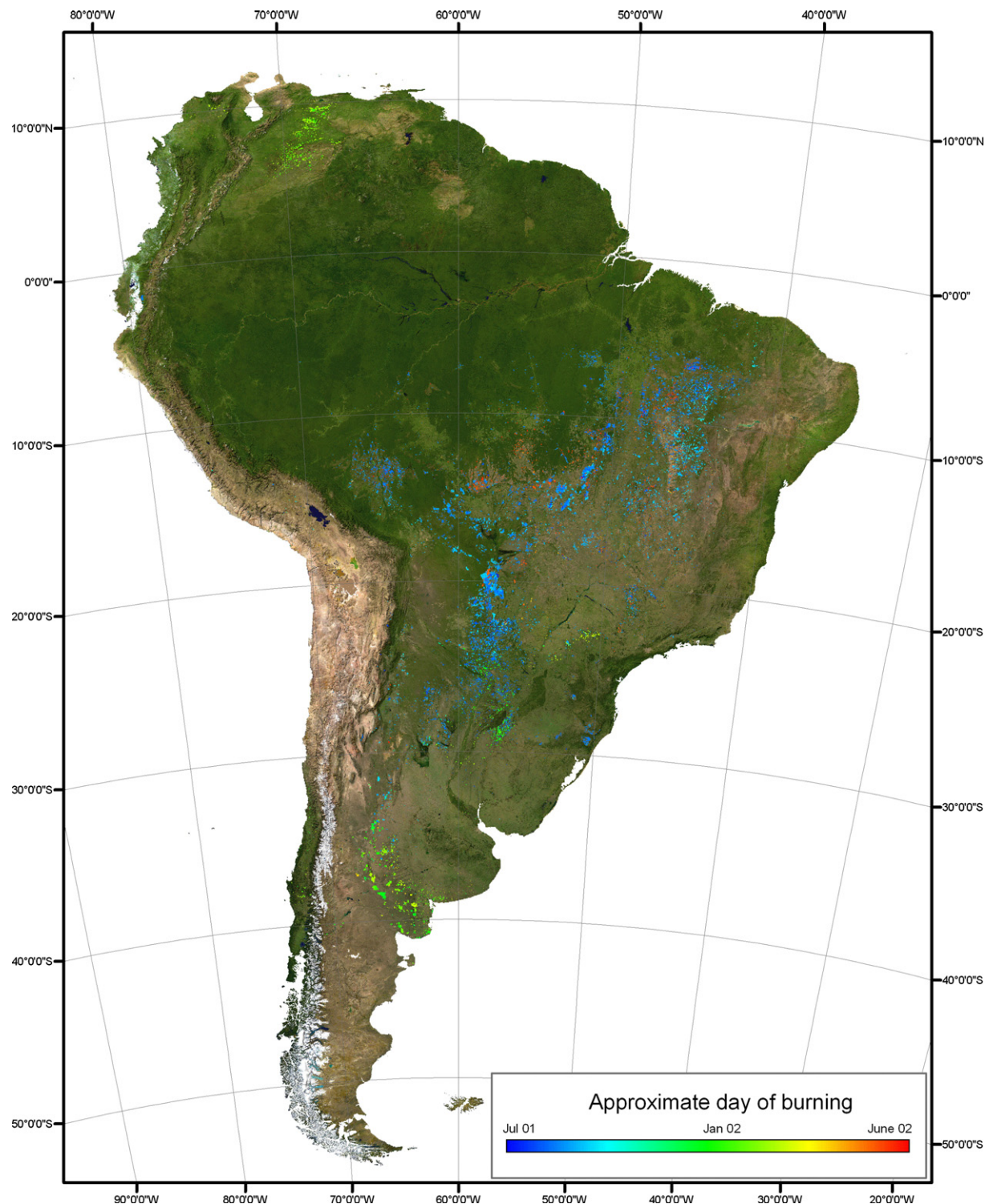


**Fig. 13.** South America subset of the global MODIS burned area product, for the July 2001–June 2002 period. Burned areas are displayed in a rainbow color scale according to the detection date, from blue (July 2001) to red (June 2002). To provide geographic context, the burned areas are superimposed on the NASA Blue Marble true color MODIS surface reflectance composite. Projection: Albers Equal Area Conic.

for July 2001 to June 2002 (**Table 2**) is similar to the annual 2001 and 2002 estimates of  $3.74$  and  $3.51 \times 10^6 \text{ km}^2$  respectively, reported by [Giglio et al., 2006a](#) by calibrating MODIS active fire detections to derive burned area estimates. Other available global burned area products have been generated for the calendar year 2000, and estimated total area burned as  $3.53 \times 10^6 \text{ km}^2$  ([GBA 2000](#), [Tansey et al., 2004](#)) and  $2.01 \times 10^6 \text{ km}^2$  ([Globscar, Simon et al., 2004](#)).

Cloud is the primary cause of missing data for both the MODIS active fire and burned area products. The average annual global unmapped area (the average of the black and red lines in **Fig. 4**) are 43% and 30% for the MODIS burned area and active fire products respectively, and by continent is greatest in Northern Eurasia, 68% and 50% annual average unmapped respectively (**Table 2**). Given the spatio-temporal variation in cloudiness at satellite overpass times ([Roy et al., 2006; Ju & Roy, 2008](#)) meaningful interpretation of unmapped area statistics should be more properly considered in terms of monthly data (illustrated in **Fig. 4**) and preferably for smaller regions than considered here. It is evident however, that assuming unmapped areas to be unburned is problematic, and failing to report unmapped areas when considering burned area statistics may seriously bias subsequent interpretation. Further research concerning appropriate reporting protocols is required in this respect.

The global temporal distribution of burning evident in **Fig. 4** is consistent with previous global studies ([Dwyer et al., 1998; Tansey et al., 2004; Boschetti et al. 2004; Csiszar et al., 2005; Giglio et al., 2006b](#)). The monthly variability of burning is mainly driven by burning in Africa and Australia (which account for respectively 68% and 17% of the total burned area) (**Table 2**). Global fire activity has two separate seasonal maxima: August, which is the absolute maximum, and December. These maxima correspond to the peak fire season months in the Northern Hemisphere (December) primarily due to the fire activity in Africa, and in the Southern hemisphere (August) due to a combination of the fire activity in Southern Africa and Australia.

**Fig. 5** shows global histograms as **Fig. 4** but reported for each vegetation class. The “other” class is composed of unclassified MODIS land cover product pixels and the urban and water classes that do not burn significantly. **Table 3** summarizes the results for the 12 month study period. Savannas, woody savannas, grasslands and shrublands account alone for 85% of the MODIS burned areas (over  $3.1 \times 10^6 \text{ km}^2$ ), a figure consistent but greater than with the active fires detections, which account for 73.7% (over  $2.38 \times 10^6 \text{ km}^2$ ). Conversely, the five forest classes (evergreen needleleaf, evergreen broadleaf, deciduous needleleaf, deciduous broadleaf and mixed forest) account for only 5.5% of the global MODIS burned areas ( $0.20 \times 10^6 \text{ km}^2$ ) but for 11.6% of the active fire detections (over  $0.37 \times 10^6 \text{ km}^2$ ), highlighting the fact that many forest fires are detected by the active fire product but not by the burned area product. This is in agreement with the findings reported in the previous section (**Figs. 2 and 3**), although the two fire products report the same area burned in the mixed forest class, and the MODIS burned area product detects a greater area of burned deciduous broadleaf forest. Burned cropland areas represent 7.5% ( $0.27 \times 10^6 \text{ km}^2$ ) of the total burned area product area but 12.4% of the active fire detections ( $0.40 \times 10^6 \text{ km}^2$ ), this difference may be because of a preponderance of small fires associated with agricultural practices which can be detected by the active fire product ([Korontzi et al., 2006](#)) but are too short-lived (due to post-fire land management) or too small to be detected as burned areas at the MODIS 500 m spatial resolution. This is discussed in more detail in Section 7.

### 6.2.2. Continental results

Continental monthly histograms of burned areas and active fires for the UMD vegetation classes are illustrated in **Figs. 7, 9–12 and 14**, and are discussed briefly below. In addition, illustrative annual composites of the MODIS burned area product for Africa, Australia-Oceania, and South America are shown in **Figs. 6, 8 and 13** respectively. In these three figures only the latest (most recent) day of burning is

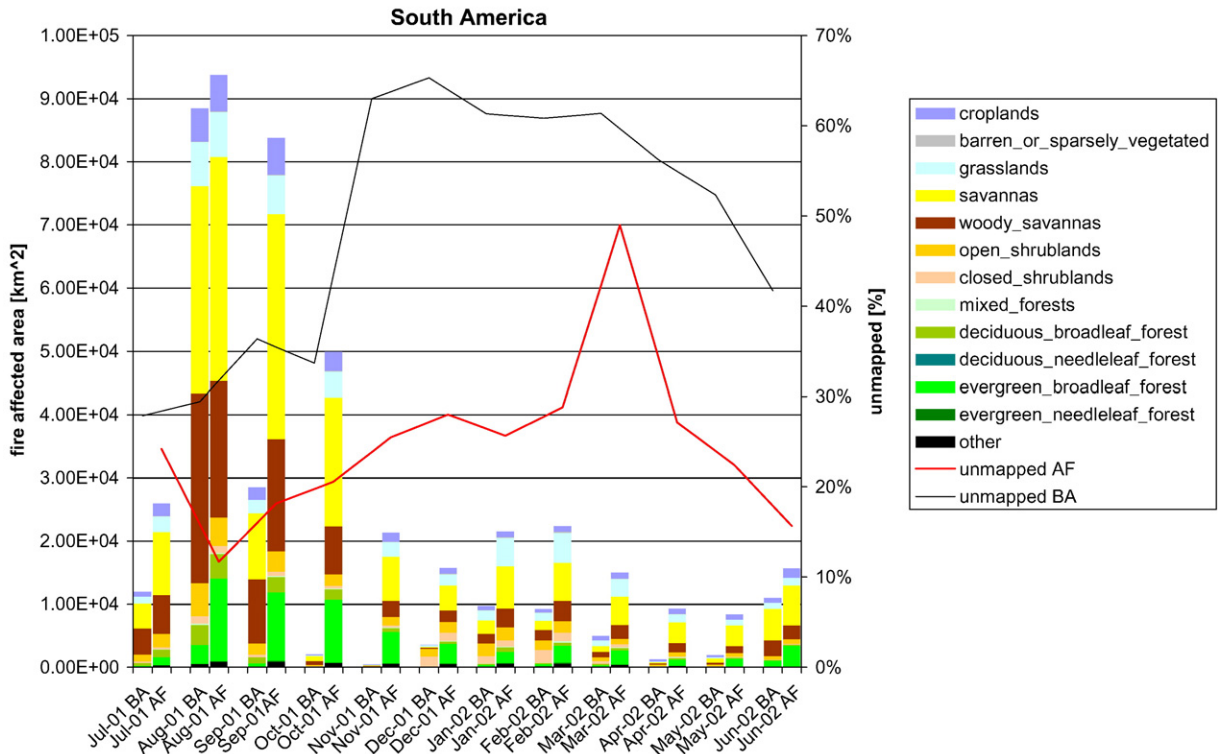


**Fig. 14.** Monthly histograms of fire affected area in South America detected by the MODIS burned area (BA) product (left bar) and the MODIS active fire (AF) product (right bar) for different MODIS vegetation classes. The black lines show, for South America, the percentage of unmapped pixels in the monthly burned area product and the red lines show, for Africa, the average of the percentage of unmapped days according to the active fire product.

shown at locations which burned more than once during the year. The burned areas are illustrated using a chronological rainbow color scheme to indicate the approximate day of burning and are overlain on a MODIS surface reflectance true color composite (Stöckli et al., 2006) to provide geographic context. These three figures were selected as they show the three continental areas most affected by fire, and the burned areas remain clearly visible in a small scale (1:35,000,000 to 1:45,000,000) image when represented at the correct level of generalization using the procedure described in Boschetti et al. (2008b).

**6.2.2.1. Africa.** Fig. 6 shows a composite of the MODIS burned area product for July 2001 to June 2002 for Africa. The extensive burning across the continent is evident; with the exception of April, Africa is the continent with the most extensive burning throughout the 12 month study period (Fig. 4). The spatial and temporal patterns (Figs. 6 and 7) are similar to those observed in previous studies (Kendall et al., 1997; Barbosa et al., 1999; Tansey et al., 2004; Roy et al., 2005b). Both Northern and Southern Africa are characterized by wet seasons and a long dry season, when most of the fire activity occurs. In much of Africa, the majority of fires are thought to be anthropogenic, lit for numerous reasons including maintaining pasture and clearing land, and a relative minority of lightning ignited fires associated with early wet-season thunderstorms (Frost, 1999).

The fire season of the Southern hemisphere starts at the beginning of May, with burning in the mosaic of forest, woody savanna and savannas south of the Congo Basin, and peaks in August (with over  $0.37 \times 10^6 \text{ km}^2$  detected), moving progressively south with widespread burning in savannas and woody savannas (Fig. 7). As previously observed by Pereira et al. (1999) with AVHRR data and by Eva and Lambin (1998a) with ATSR data, the fire season north of the Congo Basin has a symmetric behavior, starting in October at the interface between savannas/shrublands and forest, and moving progressively North through the Sudanian zone towards the Sahel, reaching its peak in December, with over  $0.48 \times 10^6 \text{ km}^2$  detected by the MODIS burned area product and  $0.28 \times 10^6 \text{ km}^2$  detected by the MODIS active fire product.

**6.2.2.2. Australia-Oceania.** Fig. 8 shows a composite of the MODIS burned area product for July 2001 to June 2002 for Australia-Oceania. This continent is the second largest contributor to biomass burning after Africa (Table 2). The fire season starts with the dry season in the summer months at the start of the year, reaching a peak in September and declining in December (Fig. 9). The fire season starts in the northern part of Australia, and then moves to central regions (Russell-Smith et al., 2003, 2007). Fire in Australia spreads quickly and, with a relatively homogeneous landscape and no natural barriers, affects very large areas. Individual burned areas can cover hundreds, or even thousands, of square kilometers (Williams et al., 2002; Russell-Smith et al., 2003). When this occurs, the frequency of the MODIS overpass is usually insufficient to sample adequately the progression of the fire front, as reflected by the discrepancy between the MODIS burned area product ( $6.32 \times 10^5 \text{ km}^2$ ) and the active fire product ( $3.87 \times 10^5 \text{ km}^2$ ) (Table 2). This difference is marked in the three vegetation classes most affected by fire (open shrublands, savannas and grasslands), while the estimates are similar for wooded savannas, and higher for the active fire product in the forest classes ( $13.7 \times 10^4 \text{ km}^2$  in the active fire product versus  $6.97 \times 10^3 \text{ km}^2$  in the burned area product aggregated over all forest classes for the whole year).

**6.2.2.3. Northern and Southern Eurasia.** The majority of burning in Northern Eurasia occurred in croplands with a peak in August (Fig. 10). Large areas of burning were detected in Italy, the Balkans and north of the Black Sea, accounting for  $0.05 \times 10^6 \text{ km}^2$ , in good agreement with the number of active fires (Fig. 10) and with previous analyses of agricultural burning patterns (Korontzi et al., 2006). Burning in savannas, shrublands and forest occurred between May and Septem-

ber. In the forest classes the burned area product had considerably fewer detections than the active fire product (about  $10.10 \times 10^3 \text{ km}^2$  versus  $30.23 \times 10^3 \text{ km}^2$  aggregating all the forest classes). These figures are in line with the yearly estimates ( $20 \times 10^3$  to  $55 \times 10^3 \text{ km}^2$ ) reported by Isaev et al. (2002) for Siberia alone, derived from national inventory data, and with the  $27 \times 10^3 \text{ km}^2$  estimated by Bartalev et al. (2007) for the summer of 2001 from SPOT-VEGETATION data. In this period, Western Europe did not suffer from the large wildfires which occurred in particular in Mediterranean countries in the summers of 2003 and 2007 (Boschetti et al., 2008a; European Forest Fire Information System, WWW3). In general, both MODIS fire products depict a fire season coincident with the Northern Eurasian summer season. However, the high number of unmapped pixels (due primarily to clouds and snow) is such that during the winter months there is less opportunity for fire detection (missing data over 50% October to April, with 90% missing November to February).

Burning in Southern Eurasia occurs in two distinct regions. In the months June to November, fire affects mainly the grasslands of Middle East and northern China, with a significant presence of agricultural burning (Streets et al., 2003). In the first months of the year, fire is concentrated in India and in South East Asia, with burned areas in savannas, woody savannas and agricultural areas (Streets et al., 2003; Hao and Liu, 2004). These two contributions are visible in both products in Fig. 11, despite the discrepancies in estimates of the affected area: the active fire product estimate ( $2.14 \times 10^5 \text{ km}^2$ ) is about 40% higher than the burned area estimate ( $1.56 \times 10^5 \text{ km}^2$ ). The difference is mainly due to a drastic underestimation of the contribution of forest fires: throughout the year the active fire product detects a large number of fires ( $3.82 \times 10^4 \text{ km}^2$ ) in evergreen broadleaf forest, which are largely absent from the burned areas product (only  $7.17 \times 10^3 \text{ km}^2$ ). One explanation for the large discrepancy is the persistent cloud cover at the time of MODIS overpass during the fire season in South East Asia (January to April) and in Indonesia (May to October), with insufficient cloud-free data available to run the burned area algorithm.

**6.2.2.4. Americas.** Fire occurs in a range of environments in North America: from forests in Canada and in the United States (Johnston, 1996), to grasslands, Mediterranean ecosystems and agricultural areas in the continental United States and Mexico (Minnich & Chou, 1997; Fule & Covington, 1996). Only 1.1% of the total MODIS burned area detections in the period covered by this study occurred in North America (Table 2), which is also the continent with the biggest discrepancy between burned areas and active fires (Figs. 4 and 12), having approximately five times as many active fires ( $1.43 \times 10^5 \text{ km}^2$ ) than burned area detections ( $4.01 \times 10^4 \text{ km}^2$ ). Mexico is the only region of the Americas with a marked peak of active fire detections and few corresponding burned area detections: a large number of small and fragmented land use related fires in April and May (Fule and Covington, 1996; Román-Cuesta et al., 2003) are largely missing from the burned area product. The July 2001–June 2002 period covered by the present study covers the latter part of the 2001 and the beginning of the 2002 boreal forest fire season. These two fire seasons were different, with moderate fire activity in 2001 and very intense activity in 2002 (Bartalev et al., 2007). This inter-annual variability is captured by both products, although it is much more evident in the active fire product.

The burned area product reports considerably fewer detections than the active fire product in South America (Figs. 13 and 14), with  $1.72 \times 10^5 \text{ km}^2$  versus  $3.79 \times 10^5 \text{ km}^2$  respectively. The two products have a similar temporal pattern, with an annual maximum of burning in August, due to fires in savannas and woody savannas south of the Amazon Basin. Multiyear analysis of the MODIS active fires record (Giglio et al., 2006a) indicates that the 2001 season is unusual in that this maximum usually occurs in September. Fire activity in the forest classes is largely missed by the burned area product, arguably because many of the fires are related to deforestation, have small dimensions

compared to the 500 m spatial resolution of the MODIS data, and are understory fires (Cochrane & Laurance, 2002; Cochrane, 2003; Alencar et al., 2006). Conversely, extensive burning occurring in grasslands and savannas in Northern Venezuela between December and April (Sanhueza, 1991) and in savannas south of the Amazon Basin in August and September (Miranda et al., 2002; Hoffmann & Moreira, 2002) is detected by both products.

## 7. Discussion

The global scale comparison of the MODIS fire products with respect to different ranges of percent tree cover and leaf area index (LAI), and at continental scale with respect to different vegetation classes, has highlighted several issues. At the scale of the analyses, for low percent tree cover and LAI, the MODIS burned area product defines a greater proportion of the landscape as burned than the active fire product; and with increasing tree cover (>60%) and LAI (>5) the MODIS active fire product defines a relatively greater proportion. This pattern is confirmed by the product comparisons reported with respect to the MODIS land cover classes. The burned area product reports a smaller amount of area burned than the active fire product in forest ecosystems, with more than a factor of three difference globally for the evergreen broadleaf and deciduous needle leaf forest classes, and comparable areas for the mixed and deciduous broadleaf forest classes. The burned area product reports globally a greater amount of area burned than the active fire product for the non-forest classes with nearly a factor of two difference for the savanna, grassland and shrubland classes. Croplands may be an exception to this pattern, as they may have low LAI at the time of agricultural burning, and globally there were a greater proportion of croplands labeled as burned by the active fire product than the burned area product.

The reasons for the observed product differences are complex, and there certainly may be exceptions at different localities and times of year, and consequently they are discussed below in general terms only.

### 7.1. Sensor obscuration

Optically thick clouds and smoke may preclude burned area and active detection and cause significant product omission errors, but their impact depends in a complex way on the spatio-temporal variability of clouds and satellite observations (Roy et al., 2006; Giglio, 2007). The MODIS active fire product will only detect fires that are burning at the time of satellite overpass and that are unobscured by optically thick cloud or smoke; however, fires that burn across the landscape slowly relative to the satellite overpass frequency may be detected in successive orbits (Giglio, 2007). Conversely, the burned area product is insensitive to the time of satellite overpass, and may be less sensitive to cloud and smoke obscuration depending on the persistence of the obscuration relative to the persistence of the post-fire change in reflectance (Roy et al., 2005a). In this study the unmapped areas reported by both MODIS fire products were primarily due to cloud with an average annual global unmapped area of 43% and 30% for the MODIS burned area and active fire products respectively, and up to 68% and 50% annual average unmapped respectively in Northern Eurasia. These amounts are not insignificant and do not occur in the same places and times in the two products. Clearly, assuming such obscured, i.e. unmapped, areas to be unburned in either product may introduce bias in their comparison.

Ground fires may be obscured by overstory vegetation, particularly in regions with high LAI and percent tree cover. Modeling suggests that understory ground fires can be sensed under certain conditions at reflective wavelengths (Pereira et al., 2004), but given the complexity of burned area mapping algorithms and their sensitivity to input data quality, it is unknown to what degree understory fires are detected in

practice. Similarly, the ability of active fire products to detect understory fires has not been assessed systematically, although research has indicated active fire radiative power differences over boreal forests that may discriminate between crown and ground fire types (Wooster and Zhang, 2004).

### 7.2. Spatial factors

Global scale burned area products are necessarily generated from moderate or coarse spatial resolution satellite data and so burned areas that are small or spatially fragmented relative to the satellite spatial resolution may not be detected (Eva & Lambin, 1998b; Laris, 2005; Silva et al., 2005; Roy and Landmann, 2005). Active fire products detect fires in pixels with elevated temperatures but can only detect fires that are sufficiently hot and/or large depending on the sensor characteristics and the areal proportions and temperatures of the smoldering and flaming fire and the non-burning components (Robinson, 1991; Giglio et al., 1999; Giglio and Justice, 2003). The spatial distribution of active fires and of post-fire burned areas relative to MODIS observations (the projection of the instantaneous field-of-view onto the surface) is complicated because the observations overlap and vary in size across and along scan (Wolfe et al., 1998) and they rarely coincide with fire boundaries.

In this study the 500 m burned area and the 1 km active fire product pixels were assumed to be completely burned respectively, but depending on the characteristics of the active fires and burned areas relative to these resolutions this assumption may cause systematic biases. There is sparse information in the peer review literature on the areas of actively burning fires: previous work on satellite retrieval of active fire area has indicated areas of less than 10 ha up to 500 ha (Giglio and Kendall, 2001) although such retrievals are unreliable except under certain ideal conditions (Giglio and Justice, 2003). Burned areas tend to be orders of magnitude more extensive, for example, as observed in this study in the savanna systems of Australia and Southern Africa. The occurrence and spatial distribution of fire is a function of contrasting physical influences acting under different circumstances at different scales (Bond et al., 2005; Archibald et al., in press). Over small spatial extents ( $10^{-1}$ – $10^2$  m $^2$ ) fire ignition and spread are dominated by fuel type, moisture, and continuity; air temperature, humidity, wind speed, and microtopography; over larger extents ( $10^3$ – $10^4$  ha), factors, such as stand-level vegetation, macrotopography, seasonal weather and synoptic climate are important; and at regional scales ( $>10^5$  ha) decadal to millennial variations in climate and the mosaics of vegetation types are important (Falk et al., 2007). The influence of human activities, for example, in altering fuel loads and structure and increasing or suppressing fire ignitions (Archibald et al., in press), are also important but are poorly understood at the scale of this study.

### 7.3. Temporal factors

In general, burned area mapping approaches use multitemporal satellite data, which provide several advantages over single date data (Pereira et al., 1997; Roy et al., 2002a). The persistence of the post-fire signal depends on factors such as vegetation regrowth and dissipation of charcoal and ash by the elements (Pereira et al., 1997; Trigg and Flasse, 2000) and consequently burned area detection accuracy may change temporally as the spectral characteristics of vegetation and burned areas change (Roy & Landmann, 2005). Furthermore, in order to unambiguously separate burned areas from spectrally similar phenomena, burned area algorithms use temporally composited data (Chuvieco et al., 2005) or daily data to only identify burned pixels as those that exhibit persistent reflectance change (Roy et al., 2005a). Consequently, burned areas that are temporally impermanent, for example, agricultural fields that are burned and then plowed, may not be detected. The primary temporal limitation of active fire detection algorithms is that variable

satellite overpass times combined with diurnal variability in fire activity may systematically under-detect the area burned, especially in systems that burn rapidly over large areas, such as grassland and savanna systems, and in regions where active fires are short-lived and do not occur at the overpass time (Giglio, 2007).

#### 7.4. The need for burned area product validation

The above reasons for active fire and burned area product differences are complex, and without independent validation and further research cannot be precisely confirmed or negated. Inter comparison of products made with different algorithms and/or satellite data provide an indication of gross differences and, as here, insights into the reasons for the differences. However, product comparison with independent reference data is needed to determine product accuracy (Justice et al., 2000) and, combined with product quality assessment (Roy et al., 2002b), to identify needed product improvements.

A comprehensive program of MODIS burned area product validation is under development and international collaborations have been made and are sought with regional networks of fire scientists and product users. Independent reference data derived from high spatial resolution satellite data, such as Landsat, have been used extensively to validate lower spatial resolution burned area products (e.g., Barbosa et al., 1999; Fraser et al., 2000; Boschetti et al., 2006) and a MODIS burned area product validation protocol has been developed using a multi-date high spatial resolution satellite data approach (Roy et al., 2005b). Accuracy assessment of the MODIS burned area product is being undertaken to assess product accuracy over a widely distributed set of locations and time periods, i.e., to Committee on Earth Observation Satellites (CEOS) Validation Stage 2 (Morisette et al., 2006), with an emphasis on sampling a range of continentally representative conditions including where the burned area algorithm has apparent limitations, i.e., in regions with high forest cover, high LAI, and in croplands.

#### 8. Summary

In this study, the first year of data from the NASA MODIS Collection 5 burned area product was analyzed. Total annual and monthly area burned and unmapped data statistics were reported at continental and global scale, describing the timing and location of burning as indicated by land cover type, stressing the importance of accounting for unmapped data to reduce biases in burned area product reporting, and highlighting the need for MODIS burned area product validation.

In a first step towards validation, the MODIS burned area product was compared to the independently derived MODIS active fire product and the reasons for the different behavior of these two fire products over different environments discussed in terms of obscuration by cloud, smoke, and overstory vegetation, and spatial and temporal factors. The reasons for the observed product differences are complex, and require further research and independent validation data. The demonstrated complementary nature of the MODIS burned area and active fire products imply that with further research their synergistic use may provide improved burned area estimates.

The MODIS burned area product has been recently implemented in the MODIS land production system to systematically map burned areas globally for the 6 year MODIS observation record. Collection 5 is underway, reprocessing the Terra data record starting in 2000 to present. As the MODIS burned area product is generated, it is our intention to build on this study, developing and publishing a validated global multi-year assessment of area burned. The Collection 5 MODIS burned area product is available to the user community for research and applications (WWW1), any changes to the MODIS burned area product generation algorithm and product will occur as part of a future Collection 6.

#### Acknowledgements

This work was funded by NASA Earth System Science grant NNG04HZ18C. Our colleague Dr. Louis Giglio is acknowledged for his long standing work in developing, refining and maintaining the MODIS active fire product. We acknowledge the helpful comments made by the reviewers to improve this paper.

#### References

- Alencar, A., Nepstad, D., & Vera Diaz, M. del C. (2006). Forest understory fire in the Brazilian Amazon in ENSO and non-ENSO years: Area burned and committed carbon emissions. *Earth Interactions*, 10, 1–17.
- Archibald, S., Roy, D.P., Van Wilgen, B.W., Scholes, R.J. (in press). What limits fire?: An examination of drivers of burnt area in sub-equatorial Africa. *Global Change Biology*.
- Barbosa, P. M., Stroppiana, D., Grégoire, J. M., & Pereira, J. M. C. (1999). An assessment of vegetation fire in Africa (1981–1991): Burned areas, burned biomass, and atmospheric emissions. *Global Biogeochemical Cycles*, 13, 933–950.
- Bartalev, S. A., Egorov, V. A., Loupian, E. A., & Uvarov, I. A. (2007). Multi-year circumpolar assessment of the area burnt in boreal ecosystems using SPOT-VEGETATION. *International Journal of Remote Sensing*, 28, 1397–1404.
- Bond, W. J., Woodward, F. I., & Midgley, G. F. (2005). The global distribution of ecosystems in a world without fire. *New Phytologist*, 165, 525–538.
- Boschetti, L., Eva, H., Brivio, P. A., & Grégoire, J. M. (2004). Lessons to be learned form the intercomparison of three satellite-derived biomass burning datasets. *Geophysical Research Letters*, 31(21), L21501. doi:10.1029/2004GL021229
- Boschetti, L., Brivio, P. A., Eva, H., Gallego, J., Baraldi, A., & Grégoire, J. M. (2006). A sampling method for the retrospective validation of global burned area products. *IEEE Transactions on Geoscience and Remote Sensing*, 44, 1765–1773.
- Boschetti, L., Roy, D. P., Barbosa, P., Boca, R., & Justice, C. (2008a). A MODIS assessment of the summer 2007 extent burned in Greece. *International Journal of Remote Sensing*, 29, 2433–2436.
- Boschetti, L., Roy, D., & Justice, C. (2008b). Using NASA's world wind virtual globe for interactive visualization of the global MODIS burned area product. *International Journal of Remote Sensing*, 29, 3067–3072.
- Chuvieco, E., Ventura, C., Martin, M. P., & Gomez, I. (2005). Assessment of multitemporal compositing techniques of MODIS and AVHRR images for burned land mapping. *Remote Sensing of Environment*, 94, 450–462.
- Cochrane, M. A., & Laurance, W. F. (2002). Fire as a large-scale edge effect in Amazonian forests. *Journal of Tropical Ecology*, 18, 311–325.
- Cochrane, M. A. (2003). Fire science for rainforest. *Nature*, 421, 913–919.
- Crutzen, P. J., & Andreae, M. O. (1990). Biomass burning in the tropics: Impact on atmospheric chemistry and biogeochemical cycles. *Science*, 250, 1669–1678.
- Csiszar, I., Denis, L., Giglio, L., Justice, C. O., & Hewson, J. (2005). Global fire activity from two years of MODIS data. *International Journal of Wildland Fire*, 14, 117–130.
- Curran, P. J., & Hay, A. M. (1986). The importance of measurement error for certain procedures in remote sensing at optical wavelengths. *Photogrammetric Engineering and Remote Sensing*, 52, 229–242.
- Denman, K. L., Brasseur, G., Chidthaisong, A., Ciais, P., Cox, P. M., Dickinson, R. E., et al. (2007) Couplings between changes in the climate system and biogeochemistry. In Solomon, S., Qin, D., Manning, M., Chen, Z., Marquis, M., Averyt, K.B., Tignor, M. & Miller, H.L. (Eds) Climate Change 2007: The Physical Science Basis. Contribution of Working Group I to the Fourth Assessment Report of the Intergovernmental Panel on Climate Change. Cambridge University Press, Cambridge, United Kingdom and New York, NY, USA.
- Dwyer, E., Grégoire, J. M., & Malingreau, J. P. (1998). A global analysis of vegetation fires using satellite images: Spatial and temporal dynamics. *Ambio*, 27, 175–181.
- Eva, H., & Lambin, E. F. (1998a). Burnt area mapping in Central Africa using ATSR data. *International Journal of Remote Sensing*, 19(18), 3473–3497.
- Eva, H., & Lambin, E. F. (1998b). Remote sensing of biomass burning in tropical regions: Sampling issues and multisensor approach. *Remote Sensing of Environment*, 64, 292–315.
- Falk, D. A., Miller, C., McKenzie, D., & Black, A. E. (2007). Cross-scale analysis of fire regimes. *Ecosystems*, 10, 809–823.
- FAO (2007). Fire management global assessment 2006, 2007, FAO Forestry Paper No. 151, Rome.
- Fernandes, R., & Leblanc, S. G. (2005). Parametric (modified least squares) and non-parametric (Theil-Sen) linear regressions for predicting biophysical parameters in the presence of measurement errors. *Remote Sensing of Environment*, 95, 303–316.
- Fraser, R. H., Li, Z., & Cihlar, J. (2000). Hotspot and NDVI differencing synergy (HANDS): A new technique for burned area mapping over boreal forest. *Remote Sensing of Environment*, 74, 362–376.
- Friedl, M. A., McIver, D. K., Hodges, J. C. F., Zhang, X. Y., Muchoney, D., Strahler, A. H., et al. (2002). Global land cover mapping from MODIS: Algorithms and early results. *Remote Sensing of Environment*, 83, 287–302.
- Frost, P. G. H. (1999). Fire in southern African woodlands: origins, impacts, effects, and control. In Proceedings of an FAO meeting on public policies affecting forest fires. FAO Forestry Paper, 138.
- Fule, P. Z., & Covington, W. W. (1996). Changing fire regimes in Mexican Pine Forests: Ecological and management implications. *Journal of Forestry*, 94, 33–38.

- Giglio, L. (2007). Characterization of the tropical diurnal fire cycle using VIRS and MODIS observations. *Remote Sensing of Environment*, 108, 407–421.
- Giglio, L., Descloitres, J., Justice, C. O., & Kaufman, Y. J. (2003). An enhanced contextual fire detection algorithm for MODIS. *Remote Sensing of Environment*, 87, 273–282.
- Giglio, L., & Justice, C. O. (2003). Effect of wavelength selection on characterization of fire size and temperature. *International Journal of Remote Sensing*, 24(17), 3515–3520.
- Giglio, L., & Kendall, J. D. (2001). Application of the Dozier retrieval to wildfire characterization – A sensitivity analysis. *Remote Sensing of Environment*, 77, 34–49.
- Giglio, L., Kendall, J. D., & Justice, C. O. (1999). Evaluation of global fire detection algorithms using simulated AVHRR infrared data. *International Journal of Remote Sensing*, 20(10), 1947–1985.
- Giglio, L., van der Werf, G. R., Randerson, J. T., Collatz, G. J., & Kasibhatla, P. S. (2006a). Global estimation of burned area using MODIS active fire observations. *Atmospheric Chemistry and Physics*, 6, 957–974.
- Giglio, L., Csizsar, I., & Justice, C. O. (2006b). Global distribution and seasonality of active fires as observed with the Terra and Aqua MODIS sensors. *Journal of Geophysical Research – Biogeosciences*, 111, G02016. doi:10.1029/2005JG000142
- Hansen, M. C., DeFries, R. S., Townshend, J. R. G., & Sohlberg, R. (2000). Global land cover classification at the 1 km spatial resolution using a classification tree approach. *International Journal of Remote Sensing*, 21, 1331–1364.
- Hansen, M. C., DeFries, R. S., Townshend, J. R. G., Carroll, M., Dimiceli, C., & Sohlberg, R. A. (2003). Global percent tree cover at a spatial resolution of 500 meters: First results of the MODIS vegetation continuous fields algorithm. *Earth Interactions*, 7 paper no. 10, 15 pp. [online journal].
- Hao, W. M., & Liu, M. (2004). Spatial and temporal distribution of tropical biomass burning. *Global Biogeochemical Cycles*, 8, 495–503.
- Hoffmann, W. A., & Moreira, A. G. (2002). The role of fire in population dynamics of woody plants. In P. S. Oliveira & R.J. Marquis (Eds.), *The Cerrados of Brazil: ecology and natural history of a neotropical savanna* (pp. 159–177). New York: Columbia University Press.
- Isaev, A. S., Korovin, G. N., Bartalev, S. A., Ershov, D. V., Janetos, A., Kasischke, E. S., et al. (2002). Using remote sensing to assess Russian forest fire carbon emissions. *Climatic Change*, 55, 235–249.
- Johnston, E. A. (1996). *Fire and vegetation dynamics: studies from the North American Boreal Forest*. Cambridge University Press 143 pp.
- Ju, J., & Roy, D. P. (2008). The availability of cloud-free Landsat ETM+ data over the conterminous United States and globally. *Remote Sensing of Environment*, 112, 1196–1211.
- Justice, C. O., Belward, A., Morisette, J., Lewis, P., Privette, J., & Baret, F. (2000). Developments in the 'validation' of satellite sensor products for the study of land surface. *International Journal of Remote Sensing*, 21, 3383–3390.
- Justice, C., Giglio, L., Korontzi, S., Owens, J., Morisette, J., Roy, D., et al. (2002a). The MODIS fire products. *Remote Sensing of Environment*, 83, 244–262.
- Justice, C., Townshend, J., Vermote, E., Masuoka, E., Wolfe, R., Saleous, N., et al. (2002b). An overview of MODIS Land data processing and product status. *Remote Sensing of Environment*, 83, 3–15.
- Kasischke, E. S., Christensen, N. L., & Stocks, B. J. (1995). Fire, global warming, and the carbon balance of boreal forests. *Ecological Applications*, 5, 437–451.
- Kaufman, Y. J., Justice, C. O., Flynn, L. P., Kendall, J. D., Prins, E., Giglio, L., et al. (1998). Potential global fire monitoring from EOSMODIS. *Journal of Geophysical Research [Atmospheres]*, 103, 32215–32228.
- Kendall, J. D., Justice, C. O., Dowty, P. R., Elvidge, C. D., & Goldammer, J. G. (1997). Remote sensing of fires in Southern Africa during the SAFARI 1992 campaign. In B. Van Wilgen, M. Andreea, J. Goldammer, & J. A. Lindesay (Eds.), *Fire in Southern African Savannas* (pp. 89–133). Johannesburg: Witwatersrand University Press.
- Korontzi, S., McCarty, J., Loboda, T., Kumar, S., & Justice, C. O. (2006). Global distribution of agricultural fires in croplands from 3 years of Moderate Resolution Imaging Spectroradiometer (MODIS) data. *Global Biogeochemical Cycles*, 20(2), GB2021.
- Laris, P. (2005). Spatiotemporal problems with detecting and mapping mosaic fire regimes with coarse-resolution satellite data in savanna environments. *Remote Sensing of Environment*, 99, 412–424.
- Masuoka, E., Roy, D. P., Wolfe, R., Morisette, J., Teague, M., Saleous, N., et al. (in press). MODIS land data products: generation, quality assurance and validation. In B. Ramachandran, C. Justice & M. Abrams (Eds.) *Land Remote Sensing and Global Environmental Change: NASA's EOS and the Science of ASTER and MODIS*. Springer Verlag, New York.
- Michel, C., Lioussse, C., Grégoire, J. M., Tansey, K., Carmichael, G. R., & Woo, J. H. (2005). Biomass burning emission inventory from burnt area data given by the SPOT-Vegetation system in the frame of TRACE-P and ACE-Asia campaigns. *Journal of Geophysical Research*, 110(D9), 2005.
- Minnich, R. A., & Chou, Y. H. (1997). Wildland fire patch dynamics in the chaparral of Southern California and Northern Baja California. *International Journal of Wildland Fire*, 7(3), 221–248.
- Miranda, H. S., Bustamante, M. C., & Miranda, A. C. (2002). The fire factor. In P. S. Oliveira & R.J. Marquis (Eds.), *The Cerrados of Brazil: ecology and natural history of a neotropical savanna* (pp. 51–68). New York: Columbia University Press.
- Morisette, J. T., Baret, F., & Liang, S. (2006). Special issue on global land product validation. *IEEE TGARS*, 44(7), 1695–1697.
- Mytheni, R. B., Hoffman, S., Knyazikhin, Y., Privette, J. L., Glassy, J., Tian, Y., et al. (2002). Global products of vegetation leaf area and fraction absorbed PAR from year one of MODIS data. *Remote Sensing of Environment*, 83, 214–231.
- Mytheni, R. B., Yang, W., Nemani, R. R., Huete, A. R., Dickinson, R. E., Knyazikhin, Y., et al. (2007). Large seasonal swings in leaf area of Amazon rainforests. *Proceedings of the National Academy of Sciences*. doi:10.1073/pnas.0611338104 March 13 2007
- Pereira, J. M. C., Chuvieco, E., Beaudoin, A., & Desbois, N. (1997). Remote sensing of burned areas: A review. In E. Chuvieco (Ed.), *A review of remote sensing methods for the study of large wildland fires. Report of the Megafires Project ENV-CT96-0256, August 1997* (pp. 127–183). Alcalá de Henares, Spain: Universidad de Alcalá.
- Pereira, J. M. C., Pereira, B. S., Barbosa, P., Stroppiana, D., Vasconcelos, M. J. P., & Gregoire, J. M. (1999). Satellite monitoring of fire in the EXPRESSO study area during the 1996 dry season experiment— Active fires, burnt area, and atmospheric emissions. *Journal of Geophysical Research*, 104(D23), 30701–30712.
- Pereira, J. M. C., Bernardo, M., Privette, J. L., Taylor, K. K., Silva, J. M. N., Sá, A. C. L., et al. (2004). A simulation analysis of the detectability of understory burns in Miombo woodlands. *Remote Sensing of Environment*, 93, 296–310.
- Rasool, S. I. (1992). Requirements for terrestrial biosphere data for IGBP core projects. *IGBP-DIS Working Paper #2*, International Geosphere Biosphere Programme Data and Information Systems, Paris, France.
- Robinson, J. (1991). Fire from space—global fire evaluation using infrared remote-sensing. *International Journal of Remote Sensing*, 12, 3–24.
- Román-Cuesta, R. M., Gracia, M., & Retana, J. (2003). Environmental and human factors influencing fire trends in ENSO and non-ENSO years in tropical Mexico. *Ecological Applications*, 13, 1177–1192.
- Roy, D. P., Giglio, L., Kendall, J. D., & Justice, C. O. (1999). A multitemporal active-fire based burn scar detection algorithm. *International Journal of Remote Sensing*, 20, 1031–1038.
- Roy, D. P., Lewis, P., & Justice, C. (2002a). Burned area mapping using multi-temporal moderate spatial resolution data — a bi-directional reflectance model-based expectation approach. *Remote Sensing of Environment*, 83, 263–286.
- Roy, D. P., Borak, J., Devadiga, S., Wolfe, R., Zheng, M., & Descloitres, J. (2002b). The MODIS land product quality assessment approach. *Remote Sensing of Environment*, 83, 62–76.
- Roy, D. P., & Landmann, T. (2005). Characterizing the surface heterogeneity of fire effects using multi-temporal reflective wavelength data. *International Journal of Remote Sensing*, 26, 4197–4218.
- Roy, D. P., Jin, Y., Lewis, P. E., & Justice, C. O. (2005a). Prototyping a global algorithm for systematic fire affected area mapping using MODIS time series data. *Remote Sensing of Environment*, 97, 137–162.
- Roy, D. P., Frost, P., Justice, C., Landmann, T., Le Roux, J., Gumbo, K., et al. (2005b). The Southern Africa Fire Network (SAFNet) regional burned area product validation protocol. *International Journal of Remote Sensing*, 26, 4265–4292.
- Roy, D. P., Lewis, P., Schaaf, C., Devadiga, S., & Boschetti, L. (2006). The global impact of cloud on the production of MODIS bi-directional reflectance model based composites for terrestrial monitoring. *IEEE Geoscience and Remote Sensing Letters*, 3, 452–456.
- Russell-Smith, J., Yates, C. P., Whitehead, P. J., Smith, R., Craig, R., Allan, G. E., et al. (2007). Bushfires 'down under': Patterns and implications of contemporary Australian landscape burning. *International Journal of Wildland Fire*, 16, 361–377.
- Russell-Smith, J., Yates, C., Edwards, A., Allan, G. E., Cook, G. D., Cooke, P., et al. (2003). Contemporary fire regimes of northern Australia, 1997–2001: Changes since Aboriginal occupancy, challenges for sustainable management. *International Journal of Wildland Fire*, 12, 283–297.
- Sanhueza, E. (1991). Effects of vegetation burning on the atmospheric chemistry of the Venezuelan Savanna. In J. S. Levine (Ed.), *Global biomass burning: atmospheric, climatic, and biospheric implications* (pp. 122–124). Cambridge: MIT press.
- Scholes, R. J., Ward, D., & Justice, C. O. (1996). Emissions of trace gases and aerosol particles due to vegetation burning in southern hemisphere Africa. *Journal of Geophysical Research*, 101, 23677–23682.
- Sen, P. K. (1968). Estimates of the regression coefficient based on Kendall's tau. *Journal of the American Statistical Association*, 63, 1379–1389.
- Siegert, F., Ruecker, G., Hinrichs, A., & Hoffman, A. (2001). Increased damage from fires in logged forests during droughts caused by El Niño. *Nature*, 414, 437–440.
- Silva, J. M. N., Sá, A. C. L., & Pereira, J. M. C. (2005). Comparison of burned area estimates derived from SPOT-VEGETATION and Landsat ETM+ data in Africa: influence of spatial pattern and vegetation type. *Remote Sensing of Environment*, 96, 188–201.
- Simon, M., Plummer, S., Fierens, F., Hoeltzemann, J. J., & Arino, O. (2004). Burnt area detection at global scale using ATSR-2: the Globscar products and their qualification. *Journal of Geophysical Research*, 109, D14, D14S02. doi:10.1029/2003JD003622, 2004.
- Stöckli, R., Vermote, E., Saleous, N., Simmon, R., & Herring, D. (2006). True color earth data set includes seasonal dynamics. *EOS Transactions, American Geophysical Union*, 87(5), 49–55.
- Streets, D. G., Yarber, K. F., Woo, J. H., & Carmichael, G. R. (2003). Biomass burning in Asia: annual and seasonal estimates and atmospheric emissions. *Global Biogeochemical Cycles*, 17(4). doi:10.1029/2002GB002024
- Tansey, K., Grégoire, J. M., Stroppiana, D., Sousa, A., Silva, J. M. N., Pereira, J. M. C., et al. (2004). Vegetation burning in the year 2000: Global burned area estimates from SPOT-VEGETATION data. *Journal of Geophysical Research*, 109, D14S03. doi:10.1029/2003JD003598
- Tansey, K., Grégoire, J. M., Defourny, P., Leigh, R., Pekel, J. F., van Bogaert, E., et al. (2008). A new, global, multi-annual (2000–2007) burnt area product at 1 km resolution and daily intervals. *Geophysical Research Letters*, 35, L01401. doi:10.1029/2007GL031567
- Trigg, S., & Flasse, S. (2000). Characterizing the spectral-temporal response of burned savannah using in situ spectroradiometry and infrared thermometry. *International Journal of Remote Sensing*, 21, 3161–3168.
- Theil, H. (1950). A rank-invariant method of linear and polynomial regression analysis. *Nederlandse Akademie Wetenschappen Series A*, 53, 386–392.
- Vermote, E. F., El Saleous, N. Z., & Justice, C. O. (2002). Operational atmospheric correction of the MODIS data in the visible to middle infrared: first results. *Remote Sensing of Environment*, 83, 97–111.
- Van Der Werf, G. F., Randerson, J. T., Giglio, L., Collatz, G. J., Kasibhatla, P. S., & Arellano, A. F. (2006). Inter-annual variability in global biomass burning emissions from 1997 to 2004. *Atmospheric Chemistry and Physics*, 6, 3423–3441.

- Van Wilgen, B. W., Govender, N., Biggs, H. C., Ntsala, D., & Funda, X. N. (2004). Response of savanna fire regimes to changing fire-management policies in a large African National Park. *Conservation Biology*, 18, 1533–1540.
- Weber, M. G., & Flannigan, M. D. (1997). Canadian boreal forest ecosystem structure and function in a changing climate: Impact on fire regimes. *Environmental Review*, 5, 145–166.
- Westerling, A. L., Hidalgo, H. G., Cayan, D. R., & Swetnam, T. W. (2006). Warming and earlier spring increase western U.S. forest wildfire activity. *Science*, 313(5789), 940–943. doi:10.1126/science.1128834
- Williams, R. J., Griffiths, A. D., & Allan, G. E. (2002). Fire regimes and biodiversity in the wet-dry tropical landscapes of northern Australia. In R. A. Bradstock, J. E. Williams, & A. M. Gill (Eds.), *Flammable Australia: the fire regimes and biodiversity of a continent* (pp. 281–304). Cambridge, UK: Cambridge University Press.
- Wolfe, R., Roy, D., & Vermote, E. (1998). The MODIS land data storage, gridding and compositing methodology: L2 Grid. *IEEE Transactions on Geoscience and Remote Sensing*, 36, 1324–1338.
- Wolfe, R., Nishihama, M., Fleig, A., Kuyper, J., Roy, D., Storey, J., et al. (2002). Achieving sub-pixel geolocation accuracy in support of MODIS land science. *Remote Sensing of Environment*, 83, 31–49.
- Wooster, M. J., & Zhang, Y. H. (2004). Boreal forest fires burn less intensely in Russia than in North America. *Geophysical Research Letters*, 31, L20505. doi:10.1029/2004GL020805
- WWW1, <http://modis-fire.umd.edu/MCD45A1.asp>, MODIS Fire website, last accessed December 20th 2007.
- WWW2, <http://earth-info.nga.mil/publications/vmap0.html>, Vector Map (VMap) Level 0 is an updated and improved version of the National Imagery and Mapping Agency's (NIMA) Digital Chart of the World, last accessed December 20th 2007.
- WWW3, <http://effis.jrc.it/Home/>, European Forest Fire Information System — EFFIS, Web Site, last accessed December 20th 2007.